AN ABSTRACT OF THE THESIS OF

SCOTT ALAN FREEBURN (Name) for the degree of MASTER OF SCIENCE (Degree)

in MECHANICAL ENGINEERING (Major) presented on March 17, 1976 (Date)

Title: COMBUSTION GAS EMISSIONS SPECTRA OF OTTO CYCLE ENGINE OPERATING ON H_2, CO, AND GASOLINE USING A CALIBRATED VIDICON DETECTOR SPECTROMETER

Abstract approved: Redacted for Privacy

Professor John G. Mingle

The capabilities of the Tektronix Model J2C/7J20 Rapid Scanning Spectrometer for the determination of molecular species resulting from Otto cycle combustion were experimentally investigated after a literature search of the subject area. Combustion of hydrogen-air, carbon monoxide-air, and gasoline-air mixtures in the combustion chamber of a Cooperative Fuel Research engine was observed using a quartz window and glass fibre optic light path. Various fuel-air ratios were tested for each fuel. The experimental work indicated that the Tektronix unit was well adapted to monitoring the rapidly changing light emissions and for rapid searches of the spectrum for any spectral features of interest. Only emissions from CO, CO_2, and H_2O were identified with certainty as the band spectra of these molecules masked emissions of other species thermodynamically predicted to exist.

An improved optical connection and a light gating system are suggested as means to improve the instrument's resolving power for this application.

Combustion Gas Emissions Spectra of Otto Cycle Engine Operating on H_2, CO, and Gasoline Using a Calibrated Vidicon Detector Spectrometer

By

Scott Alan Freeburn

A THESIS

submitted to

Oregon State University

in partial fulfillment of
the requirements for the
degree of

Master of Science

June, 1976

APPROVED:

Redacted for Privacy

Professor of Mechanical Engineering

Redacted for Privacy

Head of Department of Mechanical Engineering

Redacted for Privacy

Dean of Graduate School

Date thesis is presented March 17, 1976

Typed by Terri Sylvester for Scott Alan Freeburn

ACKNOWLEDGMENTS

I wish to thank Dr. R. W. Boubel for his assistance in this thesis and in my entire graduate program. I wish also to thank him for the opportunities he has provided me both inside and outside my academic endeavors.

My thanks to Professor J. G. Mingle for his assistance in starting this thesis and his encouragement and understanding in completing it.

Thanks to Jere Marrs, and especially Ed Caryl of Tektronix, Inc. for all their technical assistance and to Tektronix, Inc. for use of the Rapid Scanning Spectrometer.

Many thanks to Terri Sylvester for her diligent secretarial help and suggestions.

Thanks to Paula and Bernie Banks for their special assistance with the photographic work.

My wife, Nancy, deserves special thanks for her help and undying patience.

S.A.F.

TABLE OF CONTENTS

LIST OF FIGURES

APPENDIX FIGURES

LIST OF TABLES

APPENDIX TABLES

COMBUSTION GAS EMISSIONS SPECTRA OF OTTO CYCLE ENGINE OPERATING ON H_2, CO, AND GASOLINE USING A CALIBRATED VIDICON DETECTOR SPECTROMETER

INTRODUCTION

To further reduce the pollutant emission from the conventional automobile engine, it has become apparent that a better understanding of combustion processes is necessary. Technology has been limited by the inhospitable environment of the typical engine cylinder. High temperatures and pressures and the extremely short duration of combustion activity conspire to keep the facts of the process a secret. High speed photographic and spectrographic, inspection through quartz windows, direct gas sampling, as well as measurement of cylinder pressure, temperature, and "knock" have been useful methods for studying the combustion process and have provided the bulk of the information now available.

The Rapid Scanning Spectrometer (RSS), developed and supplied by Tektronix, Inc., used in the experimental work following offered capabilities beyond those of previously used spectrographs and monochromator-photomultiplier apparatuses. The instrument was immediately adaptable to engine combustion chambers through a quartz window-glass fibre optical connection, and automatic amplification of the optical signal by electronic means. This convenient system, as well as the instrument's compact size, seemed to indicate that the spectrometer could be used not only for research but for field work as well.

The instrument's dispersive analysis capabilities in real time indicated a versatility greater than either non-dispersive units or spectrographic analysis relying on photographic storage of data.

Purpose and Scope

It is the purpose of this work to summarize some of the previous spectroscopic investigations made of Otto cycle engines and to determine the capabilities of the Tektronix Rapid Scanning Spectrometer, in its standard form, for purposes of investigation and determination of the gases in this type of engine's combustion chamber during operation. To assist in this determination, it was deemed necessary to obtain the simplest combustion spectra possible using air as the oxidizing agent and to compare such spectra with those of standard automotive fuel, gasoline. Consequently, carbon monoxide, diatomic hydrogen, and gasoline were chosen as test fuels.

BACKGROUND

Spectroscopy Basics

Since early work in spectroscopy dealt with natural light sources (the sun, stars, flames), using glass prisms to separate wavelengths, the earliest spectra were emission spectra. Experimenters found that emissions from a glowing or hot monatomic gas resulted in emission of a series of lines. If the gas involved was polyatomic a series of bands were produced by a great number of closely spaced lines. Incandescent solids produced a continuous spectrum.

It was early on noted that the lines exhibited by monatomic emission could be ordered according to mathematical formulae as first demonstrated by Balmer and Rydberg. Rydberg was able to fit the hydrogen spectra lines to the formula:

$$\frac{1}{\lambda vac} = \bar{\nu} = R_H \left(\frac{1}{(n_1)^2} + \frac{1}{(n_2)^2} \right)$$

where λvac is the emission wavelength in a vacuum, $\bar{\nu}$ is the wave number, R_H, the Rydberg constant for hydrogen, and n_1 and n_2 positive integers ($n_2 > n_1$). As n_1 and n_2 become larger, it can be seen that the successive wave numbers $\bar{\nu}$ and, therefore, spectrum lines become very close together. A series limit is computed by allowing n_2 to become infinity.

In more complex atoms, each spectral line defined by the Rydberg formula has, associated with it, other line series. Historically, the names principal, sharp, diffuse, and fundamental were applied to these series.

A development of the Rydberg formula for predicting wave numbers in these more complex atoms is given by:

$$\bar{\nu}_n = \bar{\nu} - \frac{R_A}{(n-\Delta)^2}$$

$\bar{\nu}$ = series limit

R_A = Rydberg constant for element A

n = integer (the principal quantum number)

Δ = quantum defect number

by letting the series limit be defined by:

$$\bar{\nu} = \frac{R_A}{(n - \Delta)^2}$$

then

$$\bar{\nu}_n = R_A \left[\frac{1}{(n_1-\Delta_1)^2} + \frac{1}{(n_2-\Delta_2)^2}\right]$$

The position of sharp, principal, diffuse and fundamental lines evident in atomic transitions can, therefore, be predicted. Additional complication to the spectrum of an element results from opposite directions of spin of orbiting electrons.(36) Close examination of alkali element spectra indicate each line to be a closely spaced doublet resulting from the slightly different energy levels associated with each direction of spin.

Progressing to divalent atoms involves further complication to the spectra. Individual series of singlet and triplet lines appear each with its principal, sharp, diffuse and fundamental groups.

Increasing the number of valence electrons produces further complication in the spectra so that for iron more than 4,000 lines are present in just the visible portion of the spectra. However, it should be noted that the wave number of each line may be predicted by the difference of two numbers as in the Rydberg formula.(35, 20)

The obvious mathematical nature of the atomic spectral lines is at least partly explained by a theory put forth by Bohr. Bohr formed two hypotheses:

1. Atoms and ions exist in discrete, stationary states with energies E_1, E_2, etc.
2. Atoms absorb and emit energy only as they change between the discrete energy levels.

The spectra of atomic sources is, accordingly, explained as follows. An atom may absorb energy by revising the position of its valence electrons to some "excited state" as compared to its original "ground state." Energy may be released by the reverse operation, that of electrons returning to the ground state.

Bohr's theory implies that such changes in energy must have finite magnitudes determined by the discrete energy levels involved. Such finite energy changes, applying Planck's formula (16),

$$E = h\nu = hc\bar{\nu} = hc/\lambda$$

where E = change in energy level,

h = Planck's constant (N·m·s)

ν = frequency (s^{1})

c = velocity of light (m/s)

$\bar{\nu}$ = wave number (m^{-1}), and

λ = wavelength (m)

result in discrete wavelengths of radiation being either absorbed or emitted. The larger the energy change the shorter the wavelength of the radiation involved.

Inefficiencies of diffraction and transmission tend to diminish this quantum effect preventing spectral emissions from being purely monochromatic and thus creating spectral lines of finite width.

Molecular Spectra

In addition to the atomic spectra originating from electronic transitions, molecular spectra show band systems due to discrete frequency vibrations along internuclear axes. The band systems consist of a band head or sharp edge the position of which is determined by the electronic energy state of the molecule. The band fades or degrades to either red or violet. The degrading area of the band is actually a series of very closely spaced lines which are distinct only under high resolution. These fine lines are a result of the discrete vibrational energy superposed on the electrical energy of the molecule. If, in the case of a diatomic molecule, the vibrations are modeled as harmonic, an equation for the energy of the molecule may be written as:

$$E = E_{electronic} + v \cdot \omega$$

where v is the vibrational quantum number and ω is a constant related to the vibrational frequency of the molecule. With some added complication, it is possible to model non-harmonic oscillations by the following:

$$E = E_{electronic} + v \cdot \omega - v^2 \cdot x\omega + v^3 \; y\omega + \cdots$$

and for a given electronic transition, the wave number of the spectrum may be given by:

$$\bar{\nu} = E'_{electronic} + v' \cdot \omega' - v'^2 \cdot x'\omega' + \cdots - (E''_{electronic} + v'' \cdot \omega'' - v''^2 \cdot x''\omega'' + \cdots)$$

where the symbols ' and " refer to the upper and lower electronic states respectively.

In addition to electronic and vibrational states, discrete rotational energy states exist and further complicate the spectral systems. The discrete energy changes, due to rotational changes, are generally small but may be mathematically described much as internuclear vibrations. The resulting closely spaced spectral lines create the band effect of diatomic molecules.(12, 14)

Continuous Spectra

Incandescent particles emit energy on all wavelengths, the classic example in combustion being the glowing carbon particle. This spectrum is added to any other spectral features that already exist often masking them. The masking effect is especially effective on the fine line structure of the rotational-vibrational spectra.(35)

Multiplicity of Reactions

When making a spectroscopic analysis of the Otto cycle combustion process, it should be realized that emitted light results from a great many types of reactions over a finite period of time. Most Internal Combustion Engine (I.C.E.) related spectroscopic work done previously has used various types of radiation choppers allowing researchers to observe very short time segments in the total combustion process. When no such light gate is employed, as in this study, light emissions begin with the pre-combustion reactions and continue through the final after-

glow stages. The overlapping energy input of all these reactions, stored on film or a vidicon tube, complicates the spectrum.

The most elementary reactions, which must take place before combustion chain reactions in air can proceed, are those involving the splitting of the diatomic elements O_2, N_2 and H_2. A third body, M, is usually involved in both the decomposition and recombination reactions to provide and absorb energy.

$$H_2 + M = H + H + M$$

$$N_2 + M = N + N + M$$

$$O_2 + M = O + O$$

The number of branched chain reactions which occur in the combustion chamber is large, particularly when the fuel is hydrocarbon in nature. Fortunately, products of interest are mainly due to a few reactions which can be enumerated.

For the case of the combustion of molecular hydrogen in air, the following reactions occur:

$$H_2 + M = H + H + M$$

$$H_2 + O = OH + H$$

$$O_2 + H = OH + O$$

$$OH + H_2 = H_2O + H$$

$$OH + OH = H_2O + O$$

$$H + OH + M = H_2O + M$$

$$H + O_2 + M = HO_2 + M$$

Six molecules and two monatomic species take part in the combustion reactions involving only hydrogen and oxygen. In addition to these reactions are those which form oxides of nitrogen:

$$N_2 + M = N + N + M$$

$$N + O + M = NO + M$$

$$N_2 + O + M = N_2O + M$$

$$NO + O + M = NO_2 + M$$

$$N + O_2 = NO + O$$

$$NO + O_2 = NO_2 + O$$

$$NO + NO = N_2O + O$$

Additional reactions occur resulting in the formation of more complex oxides of nitrogen and ammonia, however, these products are produced in very small quantities due to equilibrium considerations and are, therefore, not of significance in this work.

Reactions important in the combustion of carbon monoxide are (23, 30, 32):

$$O + O_2 + M = O_3 + M$$

$$O + CO + M = CO_2 + M$$

$$O_2 + CO = CO_2 + O$$

$$O_3 + CO + M = CO_2 + O_2 + M$$

$$O_3 + CO = CO_2 + O + O$$

$$CO_2 + O_2 = CO_2 + O + O$$

Slight reaction between atomic carbon and nitrogen form low concentrations of CN radicals in combustion but cyanogen and more complex C-N compounds are essentially non-existent.

When discussing hydrocarbon reactions in air, it is necessary to include all those elementary reactions listed above plus those involving hydrocarbon compounds. The staggering number of possible combinations is, fortunately, limited by thermodynamic considerations to the simpler

species under the operating conditions typical to I.C.E. combustion. Methane and methane-based compounds such as formaldehyde, formic acid, and performic acid are generally the result of high temperature-free radical reactions of light hydrocarbons. Important reactions in the oxidation of methane are:

$$OH + CH_4 = H_2O + CH_3$$

$$CH_3 + O_2 = HCHO + OH$$

$$OH + HCHO = H_2O + CHO$$

$$CHO + O_2 = CO + HO_2$$

$$CHO + O_2 + M = CHO_3 + M$$

$$CHO_3 + HCHO = 2\ CO + H_2O + OH$$

Completion of the above chain occurs through destruction reactions for OH, HO_2 and HCHO at the vessel walls where water and CO_2 are formed. (23)

Oxidation of more complex hydrocarbons may be systemized to a degree and, therefore, certain compound types may be assumed to occur. For instance, loss of a hydrogen atom through free radical reactions leaves the hydrocarbon susceptable to attachment by an O atom leading to aldehydic group. Aldehydes therefore appear as intermediate components in the total reaction and, consequently, could appear spectrographically.

Very low concentrations of further oxidized hydrocarbons may also be expected. Primary, secondary and tertiary peroxides have been noted (23) as well as the normal, more stable, products of hydrocarbon combustion.

Employing variations of the method of Hershey, Eberhardt and Hottel (19), equilibrium concentrations of various combustion product gases from

fuels shown were computed for the parameters used in the experimental work. The values are shown in Table I. Peak temperature and pressure estimates were calculated by conventional methods from the engine specifications and standard thermodynamic data as shown in the Appendix. (4, 22, 23, 24, 33, 37, 44)

At low temperatures ($T < 1600°K$), calculated equilibrium composition of H - O - N combustion products existing at 20.4 atm. indicated 99.9% completion of the ideal reaction.(21) For the leanest H_2-air mixture ($\Phi = 0.25$), with a maximum adiabatic flame temperature of only 1345°K, water and diatomic nitrogen should be the only expected products and, therefore, compositions for $\Phi = 0.25$ are not included in Table I. However, for combustion processes to progress, molecule splitting must occur, and, therefore, OH and O may be expected spectroscopically. In addition, thermally excited O_2, H_2, and N_2 molecule emissions could be expected.

Increasing the Φ values to 0.5 and 0.69 raises adiabatic combustion temperatures significantly and, as shown in Table I, concentrations of nitric oxide increase slightly while those of O_2 and N_2 decrease. As the concentration values indicate, radiation emitted by NO and O_2 molecules will be very small compared to those of water molecules.

The combustion of carbon monoxide results in significantly higher predicted adiabatic temperatures. This was due primarily to the richer mixtures involved. Significant departures from idealized complete combustion are noted for all Φ values. Specifically, for $\Phi = 1.00$, NO concentration is greater than one-half percent and CO nearly five percent. Diatomic oxygen is 1.124 percent of the mixture.

Table I. Equilibrium Concentrations of Combustion Products at Peak Temperature and Pressure

Fuel	Φ	Press (atm.)	Temp. (°K)	Species										
				CO_2	H_2O	CO	N_2	OH	O	H_2	O_2	H	Cgas	NO
H	.50	29	1900	------	.18928	------	.71394	.00147	.00002	.00001	.09405	.00000	------	.00122
H	.69	35	2400	------	.24668	------	.68315	.00999	.00034	.00007	.04978	.00000	------	.00925
CO	1.00	38	2700	.30618	------	.04673	.62842	------	.00051	------	.01124	------	.00000	.00692
CO	1.50	39	2700	.29506	------	.13935	.56219	------	.00016	------	.00115	------	.00000	.00209
CO	1.65	39	2700	.28020	------	.18656	.53111	------	.00011	------	.00057	------	.00001	.00143
Gasoline	0.8	47	2700	.09335	.10551	.00726	.73235	.01248	.00080	.00128	.03361	.00031	.00000	.00091
Gasoline	1.0	48	2700	.10451	.13026	.01874	.72134	.00899	.00034	.00365	.00614	.00051	.00000	.00362
Gasoline	1.2	47.5	2600	.08239	.14154	.05976	.69529	.00291	.00004	.01649	.00016	.00074	.00000	.01176

The peak temperature is essentially steady with richer mixtures with a reduction of NO, O, N_2, CO_2, and O_2. Unburned CO is, of course, present in large quantity with Φ's of 1.50 and 1.65 and would be expected to appear spectroscopically. However, since the CO and CO_2 near continuum emission bands overlap extensively, spectral changes with changing Φ would be subtle. Since a reduction in the CO_2 concentration is more than balanced by CO increases, noticeable increases in intensity can be expected in this area of the spectrum as Φ is increased.

At very rich mixtures, some carbon gas may form in the combustion chamber at very low concentrations.

Combustion of gasoline and other hydrocarbon motor fuel has been studied extensively by several authors (30, 21, 19, 9) and the calculation results of Table I were checked with data of Hottel (21) and Obert. (33)

For the Φ values selected, virtually all species noted occur to some degree in hydrocarbon combustion with exception carbon gas. Spectroscopic emissions of OH, O, and H can be expected to be severely masked due to the low concentrations of these species and the consequent emission intensities. Strong emission signals would be expected of H_2O, CO_2, and CO.

Non-Equilibrium Effects

The gas concentrations, listed above, were computed based on thermodynamic equilibrium. All thermodynamic principles are based on the notion of equilibrium states which require a finite time period to be established. In the rapidly operating internal combustion engine, time

periods are sufficiently short to limit the formation of equilibrium mixtures of gases except at peak temperature and pressure conditions. The effect is especially evident during the expansion process. The rate of change of temperature and pressure during this period is sufficiently high to cause a "freezing effect" of normal reaction events.

As an example, consider the formation of carbon monoxide from an engine operating at a stoichiometric equivalence fuel-air ratio (Φ = 1.0). Equilibrium analysis would predict a CO concentration at exhaust temperature of about 0.05 percent. However, actual exhaust gas measurements indicate about a 1.0% concentration which is much closer to the peak temperature value. The thermodynamic predictor for CO in the exhaust gas is in error by a factor of 20, nor does the reduction of CO concentration with decreasing equivalence ratio occur as rapidly as thermodynamics would predict.

Obviously, reaction rate must play an important part in production and maintenance of CO.(30, 31, 38) As a result of studies done by Starkman, Newhall, and others, it may be shown that CO concentrations in exhaust gases of fuel rich combustion are near the peak temperature concentrations while in lean mixture combustion the CO concentration more nearly approaches the equilibrium concentration expected at exhaust gas temperatures. Nitric oxide concentrations stay nearly constant throughout expansion at the peak temperature levels (30).

These non-equilibrium processes will tend to maintain CO and NO concentration at higher than equilibrium levels thus raising the time averaged concentrations. For the storing spectrometer, this increase

in average concentrations will be recorded unless a gating device is employed to severely limit the observation period. Therefore, NO and CO concentrations cannot be directly comparable with measurements of OH or other faster reacting species when using a storing spectrometer to study the rapidly operating I.C.E.

LITERATURE SEARCH

Spectroscopic analysis of internal combustion engine processes is not new. Several previous investigators have employed a variety of instruments to help uncover the combustion processes. Such endeavors have closely followed the current problems of the era. Engine knock of the spark ignition engine for many years was a prime motive of such investigation as were the complicated processes involved in diesel combustion.

Previous work in combustion gas studies using spectral techniques may be dichotomized into dispersive and non-dispersive analysis. In particular, earliest research used dispersive analysis, usually spectrographic technique, to determine gases formed in the combustion process. Once this basic groundwork was done, non-dispersive techniques, (emission and absorption monochromators usually in series with photomultiplier devices), have been used to determine the presence of specific gases.(8) In the 1960's, a concerted effort began to determine the origins of certain pollutant gases attributed to automobiles. These efforts usually employed radiation absorbtion chambers tuned to emit and receive specific wavelength radiation as would be absorbed by the gas of interest and these devices were, therefore, oriented toward non-dispersive techniques. Such chambers are, of course, the basis for most of the exhaust gas analysis instruments currently in use.

Throughout the history of spectrometers in automotive use the spectrograph, providing the permanent record of the spectrum, and the gated spectrometer have been indispensable in examining the events occurring inside the combustion chamber.

In the early '30's, Rassweiler and Withrow used high speed cinematography and spectrographic methods of studying the combustion process. The two researchers mounted the spectrograph over a transparent cylinder head. An engine synchronized, stroboscopic shutter between engine and spectrograph allowed selection of combustion events to be recorded. Thus pre-combustion, combustion, and "after-glow" reactions could be analyzed separately.

Using this apparatus, Rassweiler and Withrow were able to identify both CH and the Swan bands of C_2 in the flame front of the combustion gases. Concentrating on the after-glow gases revealed the presence of the diffuse bands (380.0 - 450.0 nm) of the CO_2 spectrum.

Ultraviolet radiation identifying OH radicals was noted in both flame fronts and post-combustion gases. Diffuse bands from 280.0 nm to 370.0 nm were not immediately identifiable, though some correlating work seemed to indicate these were due to HCO.(45, 46)

Much of the combustion process studied by Rassweiler and Withrow was compared to previous work done with flame emissions. Such comparison led the researchers to equate inner cone Bunsen burner reactions to those that exist in combustion chamber flame fronts. Other work using absorption spectroscopy to study knocking conditions indicated the presence of formaldehyde in the pre-combustion gases.(46)

A. G. Gayden, working in England, made spectrographic studies of the combustion processes. These studies were made at both high and low initial pressure and under rich, stoichiometric, and lean fuel/air ratios. Like Rassweiler and Withrow, Gayden compared constant volume

explosions to flame burning. Though he did not describe his equipment, it may be assumed to be similar to that of Rassweiler and Withrow, as were the results.

In particular, Gayden noted that explosions in rich mixtures of hydrocarbon fuels showed the strong continuous emission band of glowing solids. This was attributed to carbon particles. Thermal emissions from these particles tended to mask chemiluminescent emissions from the flame front reactions.

Burning of stoichiometric mixtures revealed strong emissions indicating burning and afterburning of carbon monoxide. With higher initial pressures, the CO bands were still present plus stronger OH radical bands. The CO spectra was noted as being closely comparable to flame emissions. Close comparison between flame emissions and lean constant volume burning was noted for OH, CH, C_2, and HCO molecules with the CH bands at 314.3 and 362.8 nm being noticeably stronger in the combustion chamber burning.(14)

Work published by Rose, Wilson, and Benedict (34) indicated that these workers used a cesium-silver oxide photoelectric tube to detect radiation from 300 to 1200 nm. The device used no monochromator or dispersive apparatus and simply indicated radiation output as received through a quartz cylinder head window. Photocell output was amplified and fed to a photographic cathode ray oscilloscope. This system would output radiation emissions as a function of time.

Agnew, et al, used a monochromator in a line-of-sight mounting to study the pre-combustion and cool flame spectra from an Otto cycle

engine.(2) The output of the monochromator activated a lead sulfide detector cell. The electrical output of the cell was fed through an amplifier and finally displayed on a cathode ray tube oscilloscope. The optical window was of calcium fluoride and the link was completed through an internally polished copper tube. All emission spectra measured were in the infrared region.

The researchers (2) operated the engine with normal fuel and flame conditions, motoring (compressing air only), and under cool flame conditions (fuel lean and motored). Emissions from normal combustion processes indicated nearly all spectral features were due to H_2O and CO_2 molecules. Motoring air through the engine gave spectral emissions indicating the presence of H_2O. Supplemental H_2O and CO_2 gas added to the airstream gave spectral displays not unlike normal flame combustion. Only the shorter wavelength (higher energy) emissions of CO_2 and H_2O were absent. Finally, cool flame burning emitted several of the noted CO_2 bands and most of the H_2O bands and, in addition, a peak was noted at 290.0 nm and tentatively identified as H_2O .

An extension of the work expanded studies into the visible and ultraviolet regions of the spectrum by suitable modifications to the monochromator. Both photomultiplier tubes and the lead sulfide detector were used in appropriate regions of the spectrum. The data obtained represented the average spectra of several combustion cycles and was obtained at the crank angle corresponding to maximum spectral intensity.

At lean fuel mixtures (Φ = 0.786) cool flame reactions were obtained using a fuel mixture of 50% diethyl ether and Isooctane. Emission bands

resulting from combustion identified the presence of formaldehyde with an underlying continuum. HCO, which was evident in flame reactions, was not identified in the pre-flame reaction spectra.(1)

Combustion of carbon monoxide and atomic oxygen in jet stirred reactions has been studied by spectroscopic means by Malti and Pratt.(25) Chemiluminescent intensity measurements were taken at the single wavelength of 350.0 nm. A prism monochromator was used in series with a photomultiplier. Recording and signal amplification capabilities were integrated into the system. Calibration was accomplished using an external calibration bulb.

The apparatus was further used to scan the combusting gases in the 300.0 to 600.0 nm range. Continuum radiation was observed from the gas between 325.0 and 425.0 nm and was thought to be due to "CO + O chemiluminescence." There was a slight "flattening" of the spectral shape with methane as fuel rather than CO. The researchers did not note formaldehyde or HCO radical band emissions though a weak CH signal was noted at 431.5 nm. Emissions due to OH were noted at about 310.0 nm. Lean combustion of H_2 showed OH emissions only and intense radiation near 600.0 nm.

As the CH_4 mixture was richened, the 431.5 nm emission line strengthened. Blue-green C_2 bands were masked by other radiation.

Experimental work accomplished by De Soete (13) and Haynes (18), et al, identifying nitrogen species in combustion products used the monochromator-photomultiplier arrangement "tuned" to the identifying wavelengths of the emitting species. Newhall, in analyzing rapidly changing gas

concentrations inside a dual spark ignition engine cylinder, used an optical window of polycrystalline magnesium oxide to allow passage of infrared radiation to a UVIR double monochromator. The monochromator employed allowed study of the 5300.0 nm rotational-vibrational emissions by use of a sodium chloride prism. Detection of nitric oxide for the single wavelength of interest was by a type ISV Indium Antimonide photovoltaic device which insured a very rapid (10^{-6} s) response to the 5300.0 nm radiation intensity changes. Output voltage of the device was displayed on an oscilloscope giving a very rapid system response. The concentration versus time displays obtained on the oscilloscope indicated the non-equilibrium rate of change of NO concentration in the combustion chamber.(31)

Norrish, using an apparatus similar to Newhall's, was able to trace the concentration changes of both OH and CH in a flash photalysis tube. Photomultiplier tubes were used in place of film in a spectrograph and output was displayed on an oscilloscope screen. Total build-up and decay periods of less than one-millisecond were thus observable.(32) By use of high and low resolution monochromators and two photomultiplier tubes Becker, et al, investigated the presence of activated OH radical in flash tube combustion of hydrocarbon fuels.(6)

Initial investigations by Marrs and Caryl (26) using the Tektronix RSS system with a borosilicate window and fibre optic connection, identified vibrational-rotational bands of OH and H_2O. It was noted that the intensity of an OH identifying peak decreased markedly at both fuel rich and lean mixtures. There was a second order peak at 847.0 nm thought to

indicate CH_2O (first order 422.0 - 424.0 nm). Trace elements were also identified.(10)

EXPERIMENTAL WORK

The Test Engine

The test engine used for the experimental work was a standard Otto cycle Cooperative Fuel Research (C.F.R.) engine. This is a constant speed variable compression ratio engine designed for fuel research. The cylinder head is equipped with four ports with removable plugs allowing access to the combustion chamber for insertion of transducers, auxiliary ignition devices, or optical tools. An elaborate fuel bowl system allows precise liquid fuel metering to establish and maintain precise fuel flow rates through the carburetor. Exceptionally heavy construction is evident throughout.(4)

The C.F.R. engine was modified in the following areas: One of the cylinder head port plugs was removed and replaced with a quartz optical window. This window is discussed later in connection with the Tektronix spectrometer itself. The window allowed the transmission of combustion radiation outside the chamber.

The carburetion system required modification in order to accept the much revised fuel system described below. A gaseous fuel carburetor with the throttle butterfly valve removed was fitted on a special mounting base. The gaseous fuel carburetor was mounted in advance of the normal C.F.R. carburetor and in place of the intake air heater supplied with the C.F.R. engine as shown in Figure 1. The air intake of the gaseous fuel carburetor was connected to an air metering system consisting of a double drum pulsation dampener fitted with an entrance nozzle as shown

Figure 1. Gaseous fuel carburetor

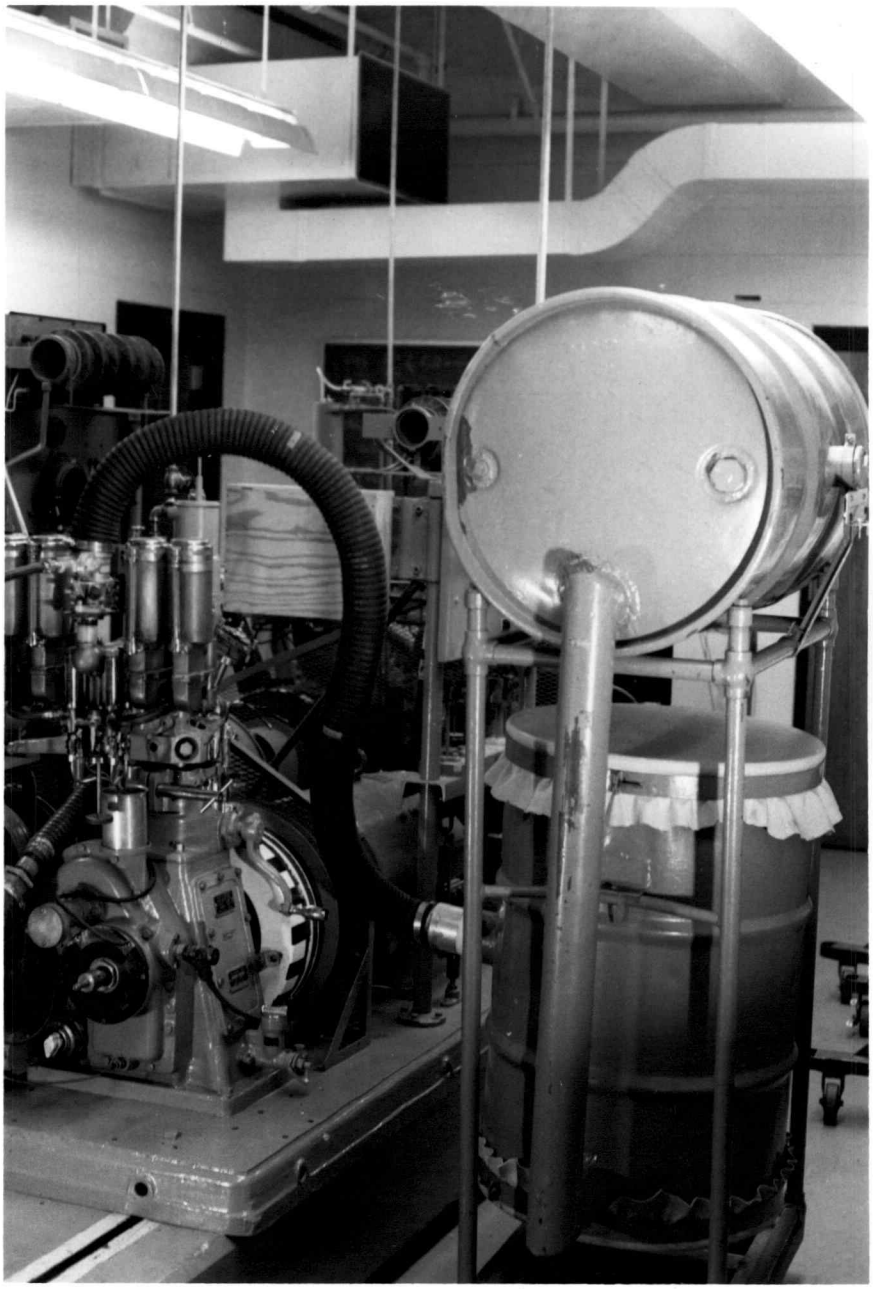

Figure 2. Assembly of CFR engine, carburetor, pulsation damper for intake air

in Figure 2. Pressure drop across the nozzle determined the air flow into the C.F.R. engine.

The Fuel System

The fuel system for the C.F.R. engine had to allow the induction of gaseous carbon monoxide and hydrogen, yet allow the normal operation on gasoline fuel. The system used was designed to allow easy changeover between different phase fuels and wide variations in flow of the gaseous fuels. In addition, accurate flow measurement of both gaseous and liquid fuels was required to obtain fuel-air ratios.

Construction of a system meeting this criteria was facilitated by use of bottled fuel gases with line pressure controlled by standard one-stage regulators typically used with gas torches. The fuel system is shown in Figure 3 and a schematic is sketched in Figure 4. Fuel gas pressure regulators were set to provide sufficient flow for maximum fuel requirements. Fuel gases flowed from the regulators to individual, globe-type metering valves through one-quarter inch plastic lines thus providing final flow rate regulation. From the metering valves, the fuel gas flowed through rotometers giving direct reading of the fuel flow rate. The gas then flowed to a three-way valve used to select either carbon monoxide or hydrogen gas which then flowed to the gaseous fuel carburetor.

It may appear that an unnecessary redundancy occurs in the use of two fuel rotometers. The rotometer deflection caused by the lower molecular weight hydrogen gas was much less than the deflection of carbon monoxide gas for identical molar flows. Since molar F/A ratios for hydrogen were less than those of CO (in order to stay below knock limits)

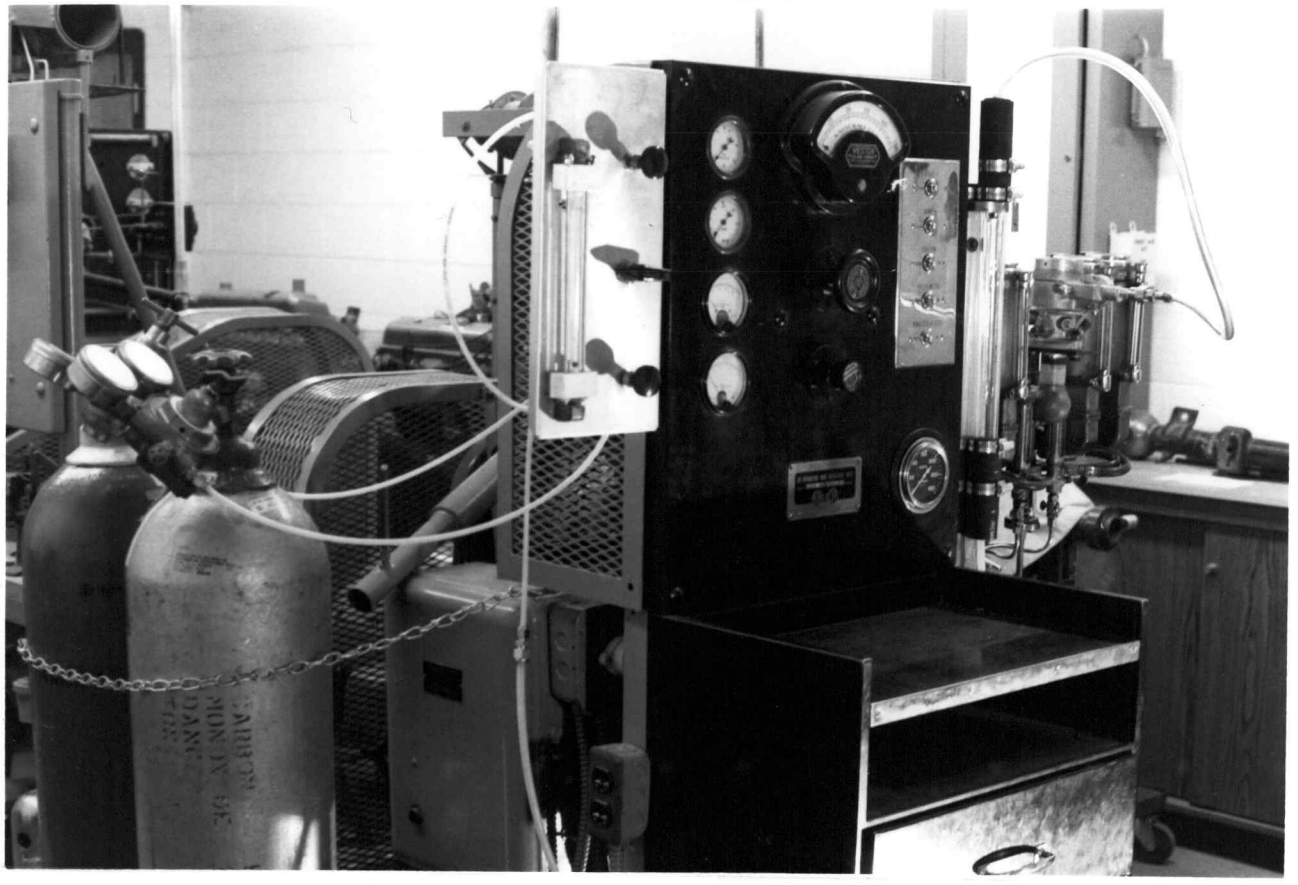

Figure 3. Assembly of fuel gas supply bottles, metering and fuel selector valve panel, and gaseous fuel flow meters.

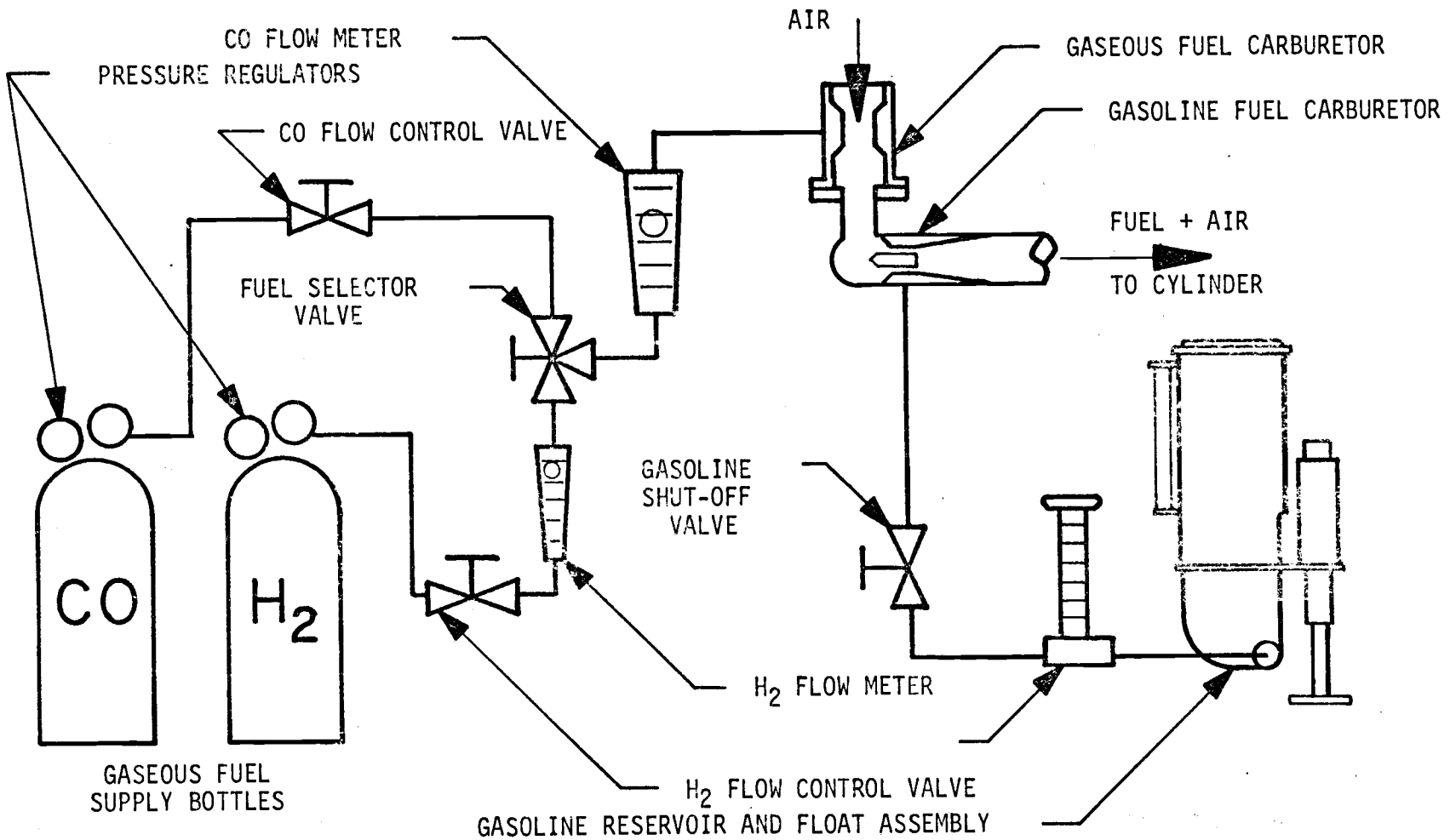

Figure 4. Schematic of gaseous and liquid fuel system.

the deflection due to hydrogen flow was reduced (in comparison to CO) even more. Consequently, a much smaller rotometer was substituted for the hydrogen "half" of the system. Thus, nearly full scale deflections were obtained in each flow meter with a consequent increase in accuracy of readings.

Rotometers meeting the requirements for gas flow were a 1.156×10^{-3} metre^3/second maximum flow rate unit for carbon monoxide and a 2.0×10^{-4} metre^3/second[1] unit for hydrogen flow measurement.

Downstream of the three-way valve, large diameter three-eighth inch tubing was used to connect to the carburetor. Short sections of one-quarter inch tube connected the flow meters to the three-way valve. The generous diameter of tubing and low restriction of gas in the gaseous fuel carburetors allowed the flow meters to be used without pressure correction. Significant pressure drops occur across the metering valves upstream of the flow meters.

Calibration of the gaseous fuel system involved measurement of both fuel flow and air flow over a range of values. This was accomplished by operating the engine at various fuel gas flow rates. Since the engine intake had no throttle plates, the total volume flow rate was constant and the fuel-air ratio would vary according to:

$$F/A \propto \frac{\delta Q_{fuel}}{\delta Q_{engine} - \delta Q_{fuel}}$$

where δQ is the volumetric flow rate. F/A values, therefore, varied predictably with changes in fuel flow rate. Therefore, setting the fuel flow determined the air flow and Φ values. Calibration curves depicting

---

[1]Flow rates are for standard air (1 atmosphere pressure and 298°K).

versus per cent flow for hydrogen and carbon monoxide are located in the Appendix.

No change in air flow was noted as gasoline flow rates were varied.

The normal C.F.R. engine fuel system and carburetor was used with gasoline. The gaseous fuel carburetor was left in place during liquid fuel test as it provided essentially no additional restriction to the air intake system and provided convenient connection to the air measurement system.

The Tektronix Spectrometer

The Tektronix J20/7J20 Rapid Scan Spectrometer is contained in two units using a glass fibre optic connection to the combustion chamber as shown in Figure 5 and 5a. The first unit of the Rapid Scanning Spectrometer system is the spectrometer itself. Optically, the spectrometer "uses a Czerny-Turner grating monochromator without an exit slit" (40) to scan the 250.0 nm to 1100.0 nm range of the unit. A schematic of a Czerny-Turner mounting is illustrated in the Appendix. In the Tektronix application, a silicon vidicon tube receives the output of the monochromator. This location is occupied by a photographic plate or the eye in a spectroscope.

The vidicon detector is composed of an array of photosensitive diodes and is able to store the dispersed spectral display, like photographic film, yet follow dynamic optical events like a photomultiplier tube. Since the vidicon target stores optical inputs, very short duration emissions may be recorded. High intensity or long duration input

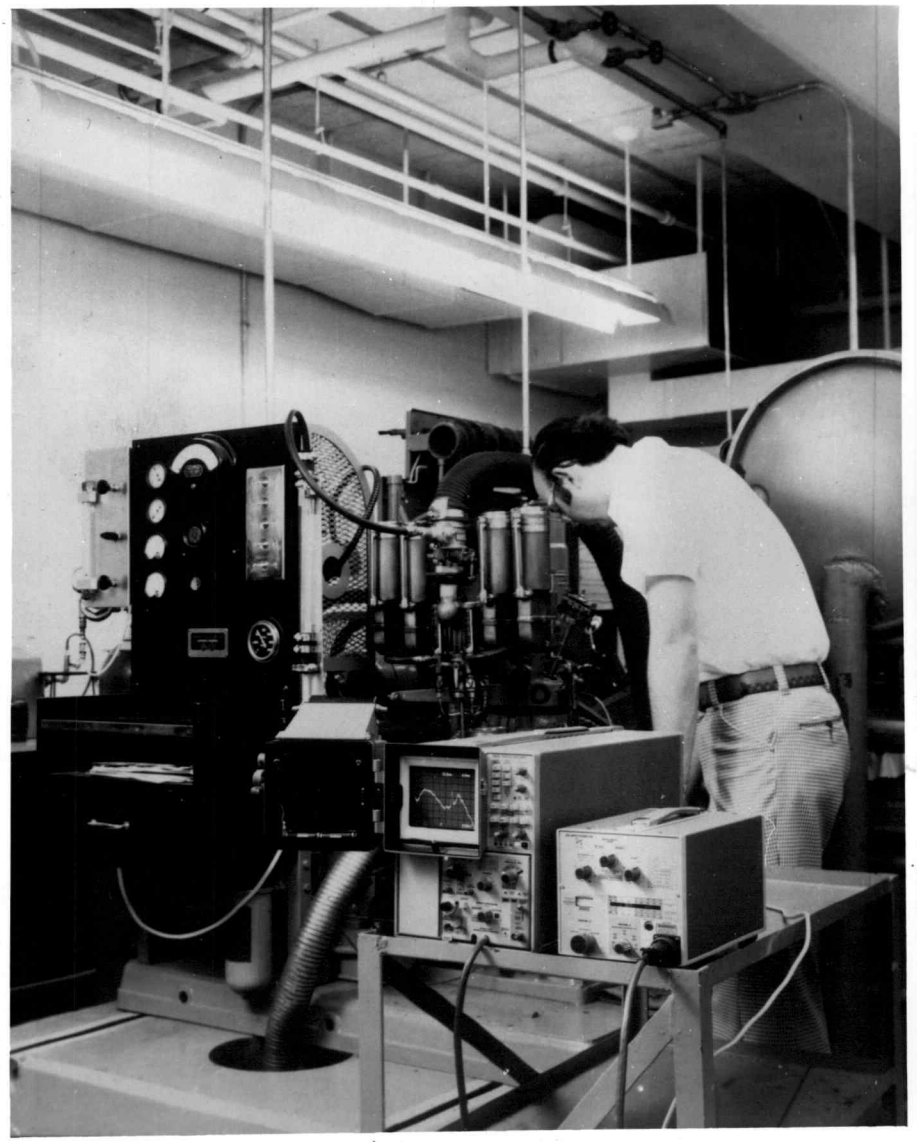

Figure 5. Spectrometer-engine arrangement

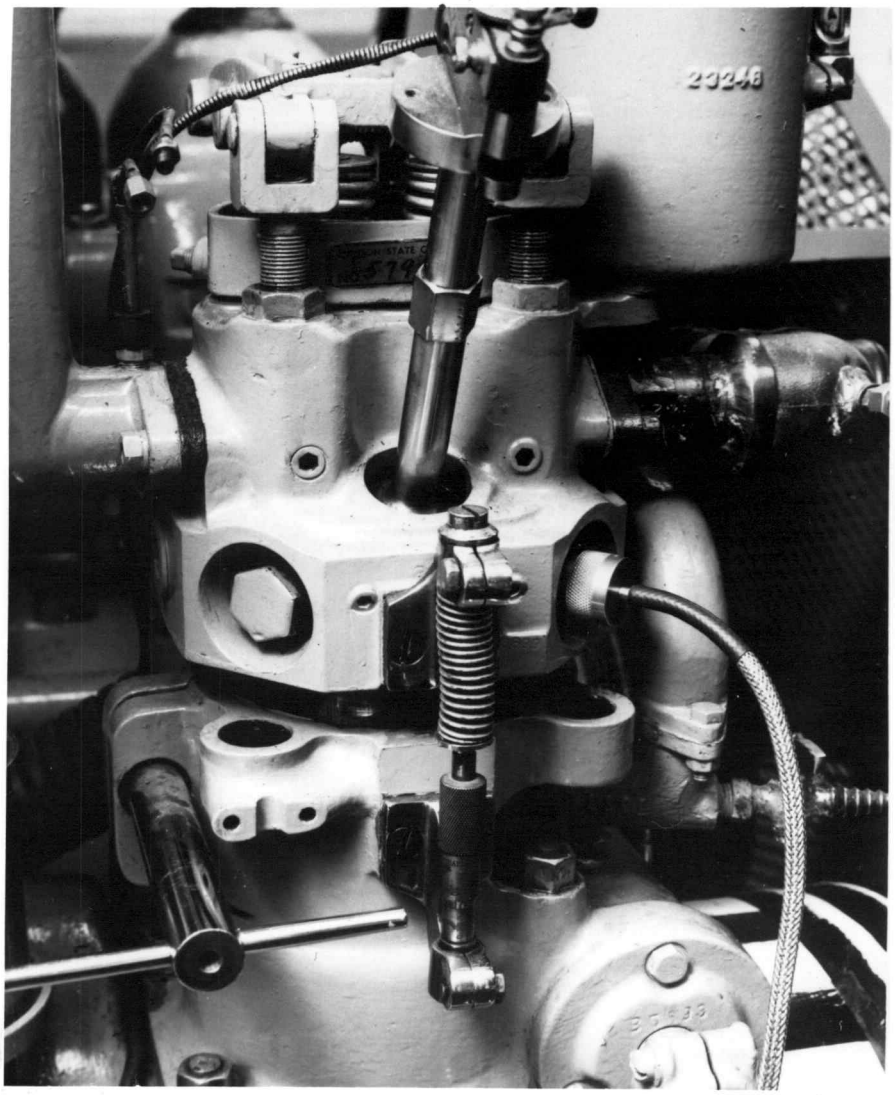

Figure 5a. Installation of quartz window and fibre optic assembly in right hand cylinder head port.

may "saturate" the photodiodes so storage efficiency begins to fall off after saturation is reached at any wavelength. Saturation was not encountered in this work due to the relatively low intensity input from the fibre optic lead.

To read what spectrum has been stored, an electron beam periodically sweeps the face of the vidicon. As the beam sweeps a location where a light signal has previously charged the tube, a small current flows indicating radiation was received at a wavelength corresponding to that position on the vidicon tube. The current flow is linearly proportional to the total optical input as long as the tube is not saturated. (16, 26)

The vidicon tube is, thus, an inherent signal integrator. All spectral inputs between electron beam sweeps are stored on the vidicon and the integrated spectrum is then read by the electron beam.(7) The sweeping electron beam reads and clears the vidicon tube in preparation for subsequent spectral inputs. (Tektronix representatives indicated that a single beam sweep generally did not completely clear the vidicon screen. Typically, three beam sweeps are required to totally clear the tube of all residual stored charge.)(29)

To increase the versatility of the spectrometer, several important features are contained in the J20. Two selectable diffraction gratings allow display of either 400 or 40 nm. Using the 40 nm grating, of course, allows greater detail and more precise identification of the wavelengths of spectral peaks. Broad range spectral inputs can be most easily examined when using the 400 nm grating.

A variable width entrance slit allows narrowing the slit to 10 μm or widening it to a "wide open" position greater than 1000 μm. Decreasing the slit width will increase spectrometer sensitivity but decrease the power of the spectral input.

A selection of filters for placement in front of the entrance slit allows calibration of the output signal, reduction in intensity (to avoid saturation), and selective screening of unwanted portions of the spectrum.

The second "half" of the RSS system is a Tektronix 7000 series oscilloscope, primarily the 7613, equipped with a 7J20 Spectrometer Plug-in unit. The 7J20 Plug-in is the complimentary unit to the J20 Spectrometer. This Plug-in allows selection of the time base for the electron beam clearing of the vidicon tube (simultaneously triggering the horizontal deflection of the C.R.T. display). It also provides the selector switch for the display dispersion, that is, the width of the section of spectrum displayed on the C.R.T.

As shown in Figure 9 through Figure 37, the oscilloscope screen is equipped with alphanumeric readout of certain instrument settings. In the upper center of the screen is noted the wavelength in nanometers at which a moveable marker dot is located and in the upper right is the width of spectrum, in nanometer, displayed between any two major graticule division. Readings in the bottom center and bottom right are the spectral sensitivity in nanowatts/nm · division and the time base sweep rate in milliseconds, respectively.

A special form of vertical gain switch allows linear, logarithmic and inverse logarithmic types of vertical deflection. The inverse logarithmic form allows use of the spectrometer for measurement of spectral absorbance. Additional controls allow internal calibration for radiometric measurements and wavelength marking.(40, 41, 42)

Combustion chamber radiation was emitted through a quartz rod-shaped "window" provided by Tektronix, Inc. Figure 6 is a cross-sectional drawing of the window. The body was made from brass hexagonal stock allowing use of hand wrenches for installation. The knurled cap could be removed after loosening the set screw and removing the fibre optic lead. The exposed "O" ring and window could then be removed for inspection and cleaning.

Transmission characteristics of the quartz window were significantly superior to those of the glass fibre optic for the wavelength scanned by the spectrometer.(3, 11)

A 60 cm fibre optic connection between combustion chamber and spectrometer provides a permanent attachment to the quartz optical port while allowing some freedom of movement of the spectrometer unit. No special alignment geometry was necessary, therefore. The fibre bundle is formed into a round cross section at the collection end to allow easy adoption to optical windows, etc. At the spectrometer end, the fibre bundle has been flattened to conform to the entrance slit dimensions. A permanent attachment was obtained after the fibre optic bundle has been aligned with the entrance slit.

Use of a fibre optic material limits the transmission of radiation to those wavelengths not absorbed by the optic material. In this work,

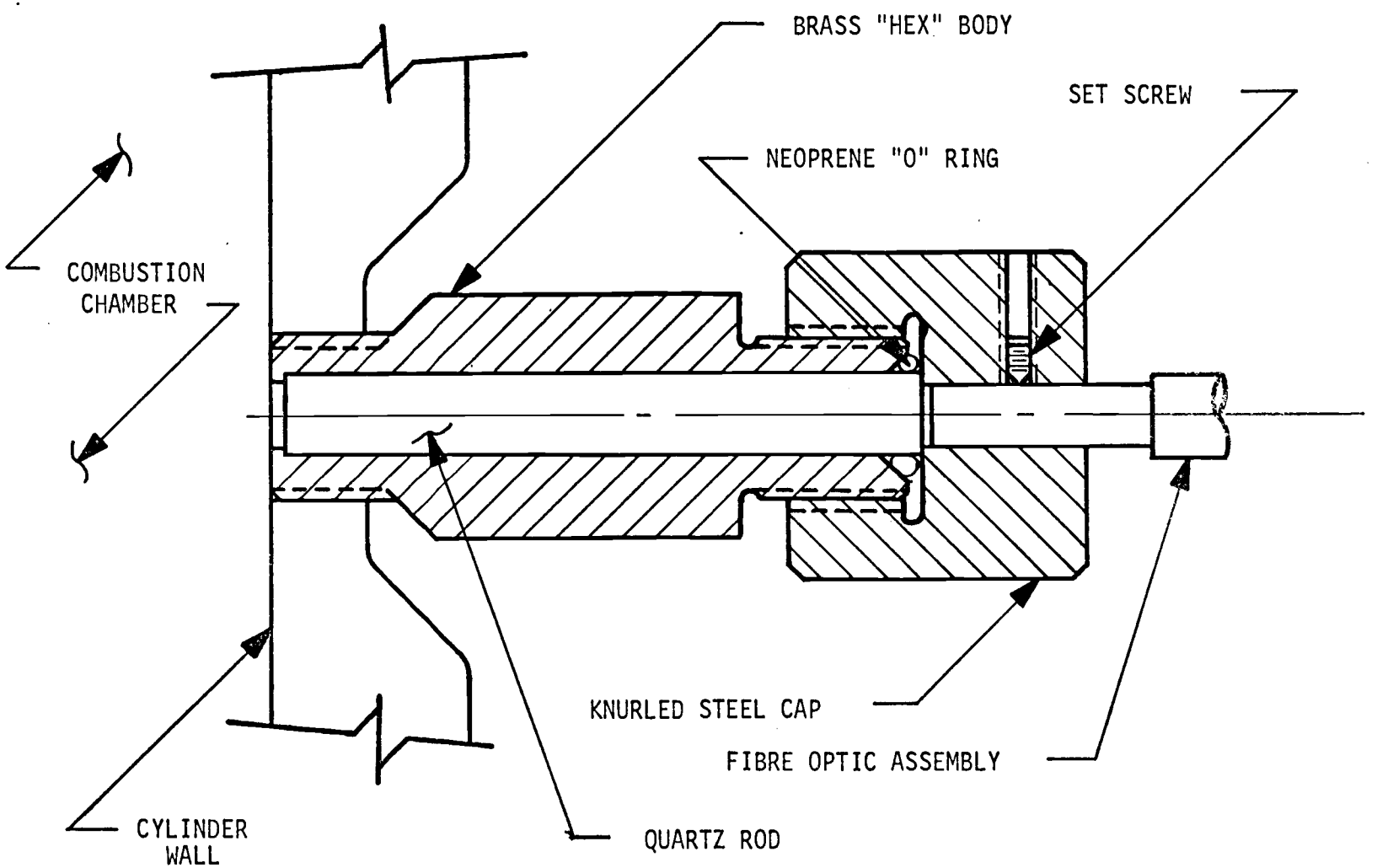

Figure 6. Quartz combustion chamber window and fibre optic assembly attachment.

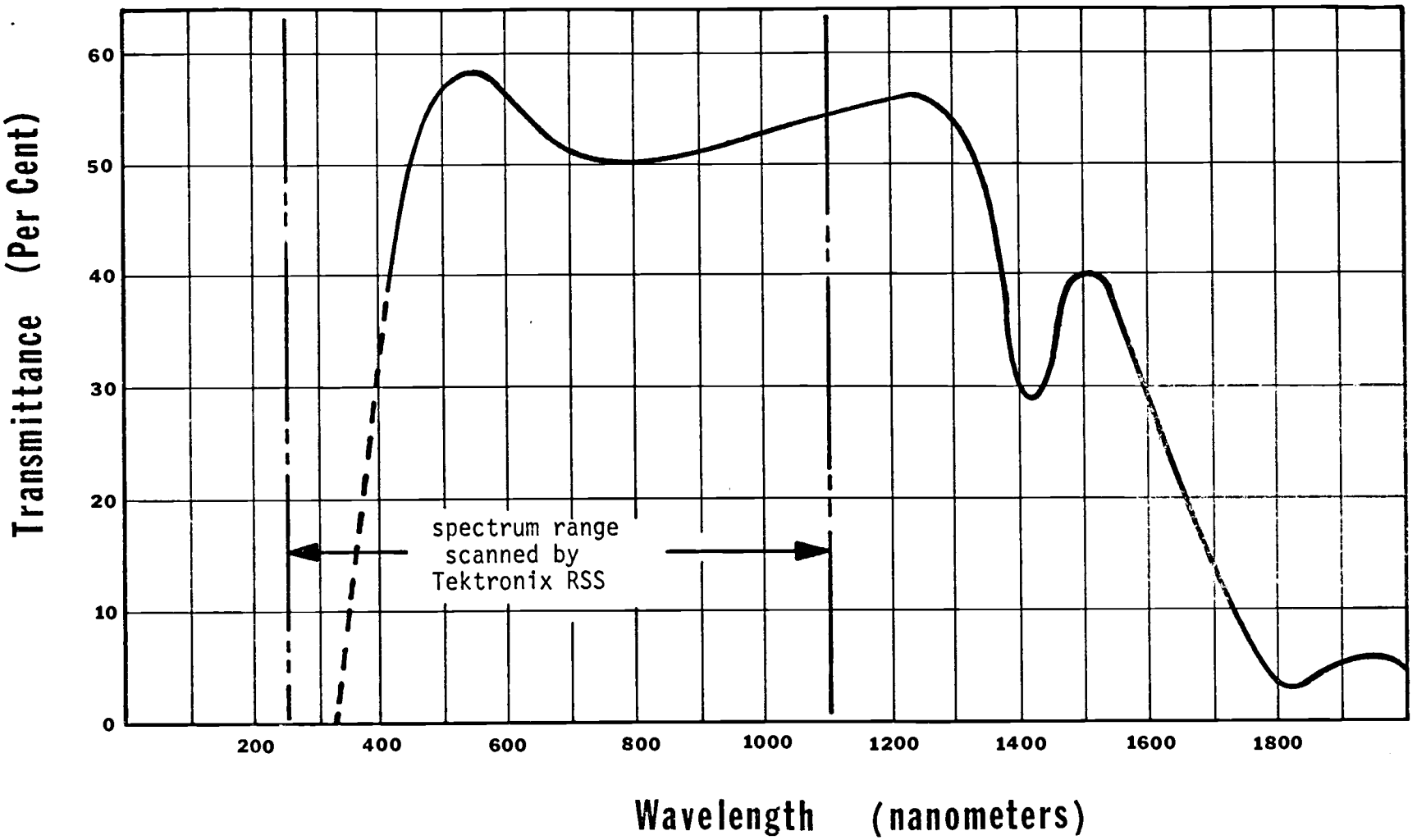

Figure 7. Transmission curve of 60 cm glass fibre optic light path. (11)

glass fibres formed the optical path. Glass is essentially opaque to radiation below 400 and above 1400 nanometers. The light transmission curve of the fibre optic bundle is shown in Figure 7.(11)

The RSS system oscilloscope is adaptable to camera use. The 35 mm camera back used in this work was mounted horizontally as shown in Figure 8. All light seals in the camera main frame unit were checked visually for leakage. To facilitate initial focusing, Tektronix supplied a ground glass screen to be placed in the film plane. The camera mount is provided with a focus adjustment knob, as shown, which was used to obtain a clear image on the glass screen. Adjustment to the screen read-out intensity and graticule lighting was made at this time also.(39)

The time per horizontal scan was selected to correspond to engine firing, and the camera shutter speed was selected such that it would include at least one beam sweep during the open shutter period. A shutter speed of one-quarter second was selected on this basis as it was the next longest time period available on the 35 mm camera back greater than the 200 ms sweep time (firing five times per second). Several test shots were taken using a Polaroid camera back and Polaroid standard ASA 3000 black and white film. From these shots and making the ASA conversion for use of Kodak Tri-X black and white (ASA 400), an aperture setting of f2.8 was selected.

Due to the relatively slow shutter speed, a cable type shutter release was employed to eliminate vibration associated with direct manual release.

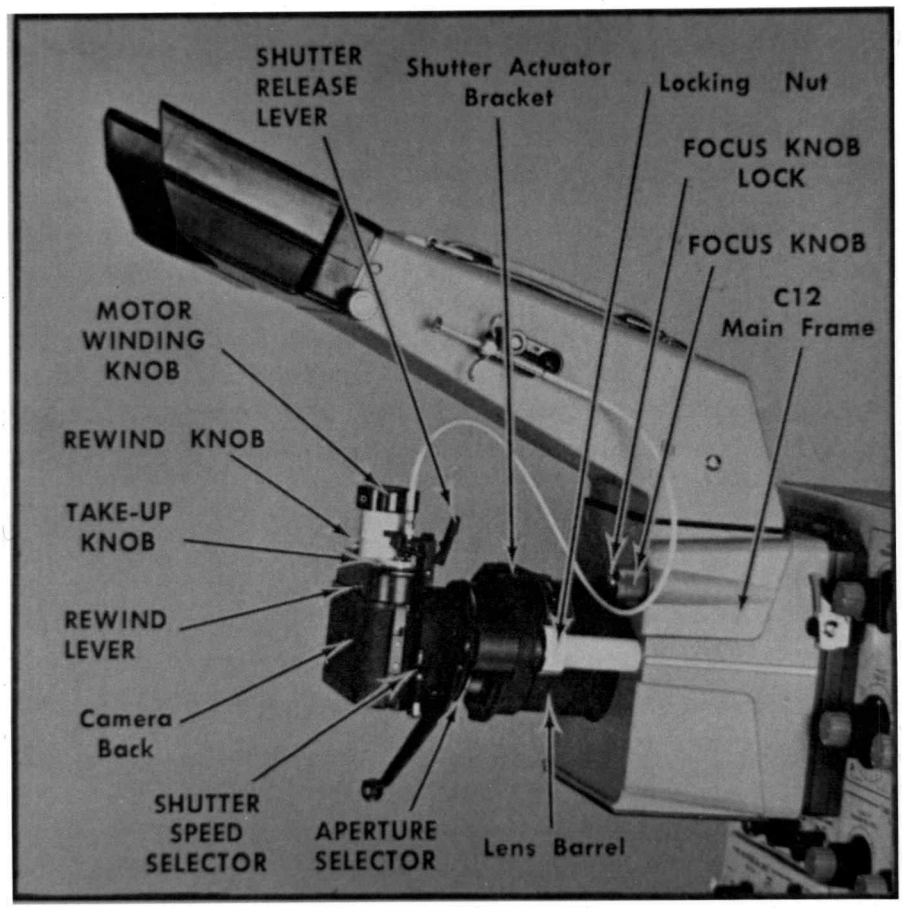

Figure 8. 35 mm camera back assembly

Experimental Procedure

After the initial set-up, the equipment was checked for operation and safety. Due to the explosive nature of hydrogen and its propensity for leakage, the room ventilating fan operated 24-hours per day during the experimentation period. (The room exhaust was located at ceiling level facilitating removal of H_2 gas which would accumulate there.) All fuel lines were checked for leaks by use of the outlet pressure gages on the regulator assemblies. If the pressure gage showed a loss in pressure after a period of time, the line connections were tightened and rechecked.

The Cooperative Fuel Research engine was started per standard procedure (4) and operated through all runs with a water jacket temperature of 210 ± 2°F. The oil heater was left at the low position resulting in approximately 130°F oil temperature during operation. No attempt was made to keep oil temperature constant.

After starting the C.F.R. engine, the RSS system was turned on. Both were allowed to warm up for twenty minutes. The engine operated on gasoline during this period, it being the least expensive fuel.

After the warm-up period, the engine was shut down and the optical window removed and cleaned with solvent. The engine was then restarted and the appropriate test fuel valve was turned on, along with the engine ignition.[2] The metering valve or fuel bowl level was adjusted for the

---

[2]Caution should be exercised at this point when using H_2 fuel. Severe knocking and intake manifold backfire occurred if the fuel-air ratio was too high ($\Phi > 0.7$). The H_2 fuel flow should be started at zero and increased slowly to the desired flow rate, unless previous runs indicate the proposed initial flow rate to be safe.

desired fuel flow for gaseous or liquid fuels respectively. Since changes in gaseous fuel flow rate severely effected the air flow rate, both fuel and air flow rates were checked for each run.

After steady state operation had been reached, the oscilloscope display is observed. Initially, for each fuel type - fuel-air ratio combination, a photographic spectral sweep was made. This procedure was followed by more photographs at higher resolution settings of those areas of the spectrum showing pronounced intensity or definable line-type spectra in the original, broad spectrum photographs. Finally, photographs were taken of specific regions in search of the identifying emissions of some molecular species predicted by the equilibrium calculations. In general, no set procedure or group of dial settings could guaranty the desired display. Since the intensity of emissions varies with the fuel input, gain settings often had to be varied to fit the display to the screen. An additional control over the input signal intensity is, of course, the slit width. Narrowing the slit not only will reduce display peak heights but also increases the resolution obtainable.

The oscilloscope time sweep was set at 200 milliseconds corresponding to the five firings per second of the 600 rpm engine. This allowed 180 milliseconds of storage time before the vidicon tube was cleared. Radiation from <u>all</u> combustion events was, therefore, stored. Sweep times as short as 10 milliseconds are possible with the J20(40), however, since the clearing of the vidicon tube is in no way chronologically tied to combustion events, outputs would be essentially random. In other

words, the instrument could read any section of the four stroke cycle, but that section would not be predictable. The "B" grating was used sparingly as it tended to be most useful for location of small peaks or for specific searches through a limited range of wavelengths. It was not useful for observing the overall display.

None of the J20's filters were used except the 500 and 800 nm monopass filters to check the calibration of the wavelength marker. This calibration was performed each time the unit was turned on and found not to vary throughout these tests. The marker read approximately 501 nm at 500 nm and 803 nm for the 800 nm monopass filter.

Throughout the testing procedure, the baseline restore mode of the instrument must be periodically activated to re-establish the zero-light reference baseline in the C.R.T. display.(40) The switch was depressed and held a few seconds before each photograph was taken. This established a consistent baseline for each data reading and eliminated the effects of display vertical drift.

With the desired display in view, the camera main frame was swung into place and latched. Figure 8 shows the camera positioned to shoot pictures. The 20 x 22 mm images of the C.R.T. screen allowed approximately 30 shots to be taken per normal 20 exposure film roll.(39) Film advance was automatic by virtue of a spring-wound drive mechanism. A near constant position near the bottom of the C.R.T. screen was chosen for the zero light trace. This allowed for maximum deflection of the output trace. (This was technically not a zero emission trace, however, as the pre-flame reactions taking place in the cylinder emitted very low

intensity radiation in the upper wavelengths recorded by the Tektronix unit. The trace obtained from this operation was, therefore, indistinguishable from a zero light trace.) Turning on the ignition then produced another trace corresponding to the emissions of the combustion process. This operation was not successful when fuel flow was modulated instead of the ignition source. Restart of the fuel flow always produced several cycles of reduced fuel input (and, therefore, reduced radiative emissions) before steady state operation was again achieved. This transient operation produced a cluttered display.

The quartz window was, of course, susceptible to deposition of combustion materials thereby reducing its transmissivity. To reduce this effect, the window was regularly removed and checked for such deposits. It was found that gasoline would satisfactorily remove all of the accumulated materials.

A photographic log book was kept to record the RSS settings and fuel-air flow data for each photograph taken. Log data included exposure number of the film roll, fuel type and flow meter readings, air flow meter readings, oscilloscope vertical gain setting, spectrometer slit width, and a column for remarks. Log tables are reproduced in the Appendix. The scale factors for scan time, marker wavelength, wavelength span, and spectral power were recorded photographically as they were displayed on the C.R.T. screen.

DISCUSSION OF TEST RESULTS

Hydrogen Fuel Emissions

Figures 9 and 10 shows the hydrogen emission spectrum for an equivalency ratio of Φ = 0.25 in the 300 - 700 nm and 700 - 1100 nm ranges respectively. Comparison with zero light curve of Figure 11 show virtually no change due ignition though oscilloscope gain is set at 20. Operation at this low fuel flow produced the onset of combustion noise but visible light was not evident through the chamber window.[3]

Increasing the equivalency ratio to Φ = 0.50 gave the first spectral change. Figure 12 shows a slight and general spectral output for the 300 - 700 nm area when compared to the zero light display of Figure 13. Figures 14 and 15 show more definite output in the 735.0 to 815.0 nm area even with a linear gain factor of only 10. The low end spectral output of Figure 12 is probably due to overlapping of some 28 O_2 vibration bands between 244.0 and 437.5 nm and approximately 50 OH vibrational bands lying between 260.8 and 352.3 nm.(17) The spectral output indicated in Figure 14 is probably due to overlapping of H_2O vibrational bands at 722.8, 795.6, and 822.7 nm.(17) Intense line spectra of oxygen are also present at 777.0 nm. Figures 16 and 17 display an obvious spectral peak at approximately 957 nm (gain set at 5) which appears to be the result of the addition of vibration-rotation bands of H_2O to the major H_2O band

---

[3]It was interesting to note that the engine was easily "throttled" simply by controlling the H_2 flow. Increasing fuel flow changed engine noise from a barely audible thump to a violent knocking explosion ultimately resulting in intake manifold backfire.

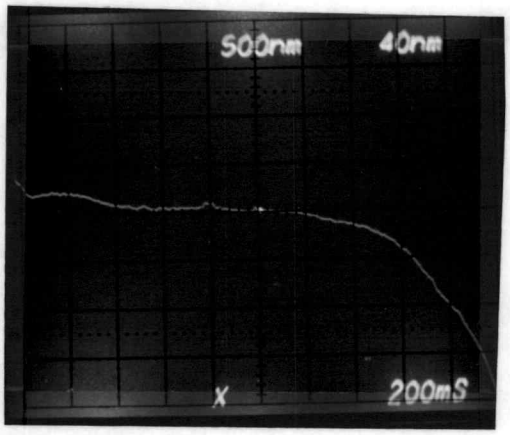

Figure 9. 300 to 700 nm emission spectrum of H_2-air combustion with ϕ = 0.25. Gain = 20.

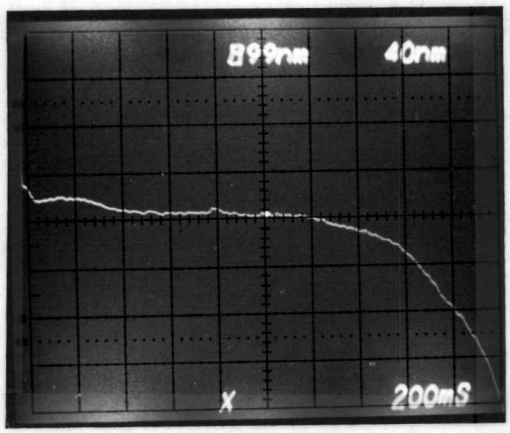

Figure 10. 700 to 1100 nm emission spectrum of H_2-air combustion with ϕ = 0.25. Gain = 20.

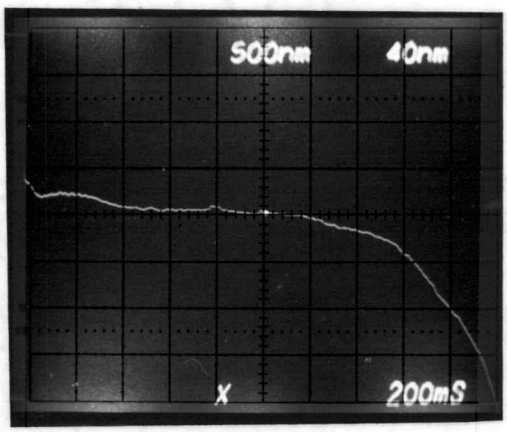

Figure 11. Zero emission trace for Figures 9 and 10.

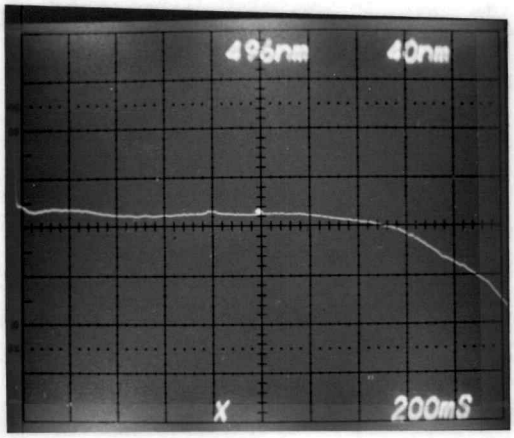

Figure 12. 300 to 700 nm emission spectrum of H_2-air combustion with ϕ = 0.50. Gain = 20.

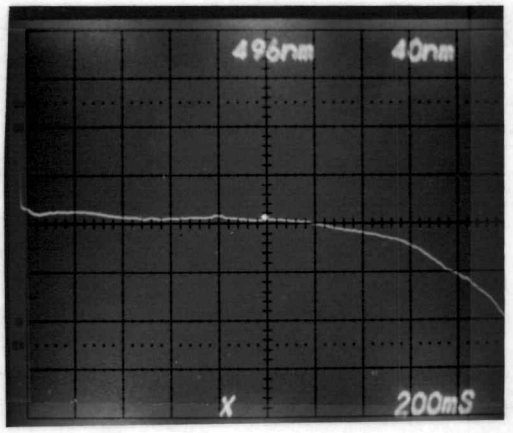

Figure 13. Zero emission trace for Figure 12.

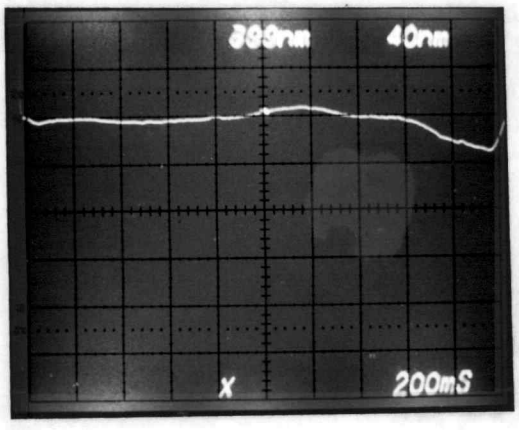

Figure 14. 500 to 900 nm emission spectrum of H_2-air combustion with ϕ = 0.50. Gain = 10.

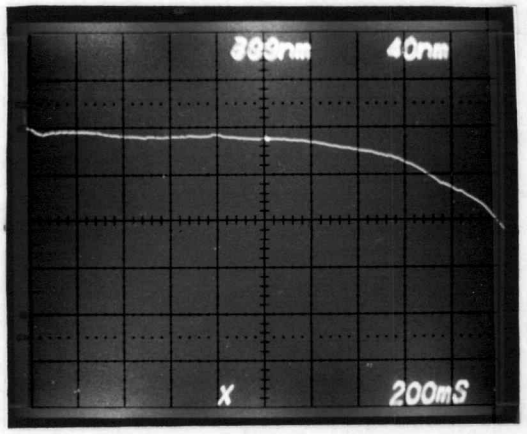

Figure 15. Zero emission trace for Figure 14.

head at 966.9 nm. Other bands heads occur at 809.7, 891.6, 927.7, and 933.3.(17) The fact that this peak was not present in Figure 10 at the lower Φ value is corroborated, to some degree, by Gayden who states the intensity of the emissions from these vibrational-rotational bands of H_2O rises rapidly with increased flame temperature.(14, 15)

The equivalency ratio was finally raised to 0.69, the upper richness limit prior to manifold backfire. As Figures 18 and 19 illustrate, there are no noticeable emissions in the ultraviolet below 400 nm, however, a broad peak has formed at 591.0 nm. The only major bands located in this section of the spectrum which might result from H_2-air combustion are again those attributable to water. Specifically band heads occur at 571.4, 591.6, 594.3, 616.5, 631.4, 645.7, and 691.9. All of these bands overlap in the region of the "peak." With increased fuel input, the magnitude of the emissions has increased as shown by Figures 20 and 21. Though the peak in Figure 21 appears nearly identical to that in Figure 16, note that the oscilloscope gain was reduced by a factor of two in Figure 21.

In reviewing the spectral display of H_2 combustion, no significant emissions were noted in the ultraviolet region below 400. nm. Emissions might be expected at 306.4 nm representing electronic transition in the OH radical, 310.4, 323.2 and 337.0 nm correlating with O_2 molecule vibrations, and the 336.0 nm vibrational band of NH radicals. In even shorter wavelengths, beyond the range of the instrument, are the NO bands. This lack of display can probably be laid to two factors. 1) At the very lean fuel settings required by the C.F.R. engine when operating on pre-

mixed hydrogen and air, peak flame temperatures do not appear to be high enough to excite the ultraviolet radiation noted (this is particularly true for the O_2 emissions), and 2) the transmissivity of the glass fibre optic material decreases significantly in the short wavelength region.

Carbon Monoxide Fuel Emissions

Photographic displays in the 300 to 700 nm range were essentially identical for CO combustion at Φ = 1.00 and 1.50 while equivalence ratios below 1.0 simply reduced spectral output. Figures 22 and 23 are for Φ = 1.00 and Figures 24 and 25 are for Φ = 1.50 and show a broad peak centered at approximately 580 nm. The peak type display may be attributed to the multibanded "Triplet System" of CO. This band system is very complex and has yet to be totally unraveled even using very high resolution spectrographs (14). Approximately 40 band heads lie between 437.4 and 646.5 nm, all bands essentially overlapping one another. In addition, another 25 band heads associated with the CO_2 molecule are located between 391.2 and 543.0 nm. This multiplicity of bands also gives high intensity in this region as verified by the vertical gain setting of only one.

The near continuum type spectrum displayed by CO combustion extends to approximately 1050.0 nm where spectral output approaches zero. These observations shown in Figures 26 and 27 and correlate well with Gaydon. (14)

Increasing the fuel rate to extremely rich mixtures (Φ = 1.65), revealed the telltale display of the carbon monoxide Triplet system. This is illustrated in Figures 28 and 29. The three peaks correspond

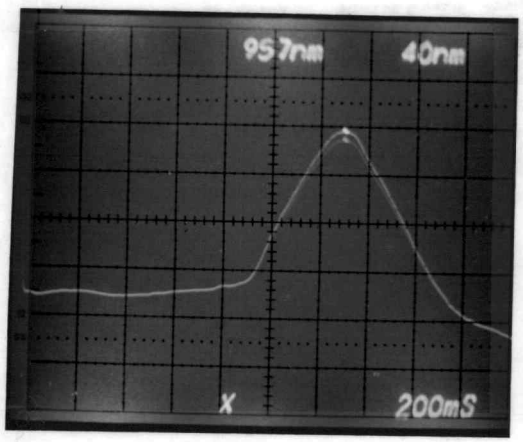

Figure 16. 700 to 1100 nm emission spectrum of H_2-air combustion with ϕ = 0.50. Gain = 5.

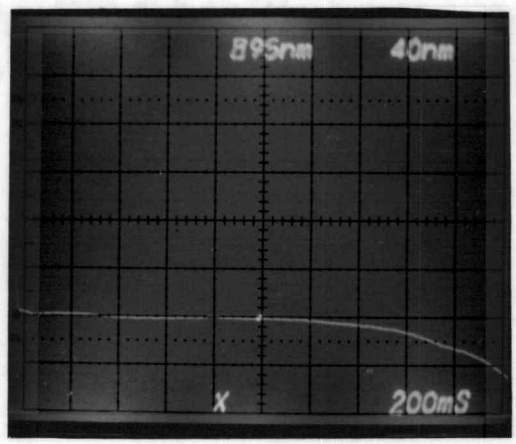

Figure 17. Zero emission trace for Figure 16.

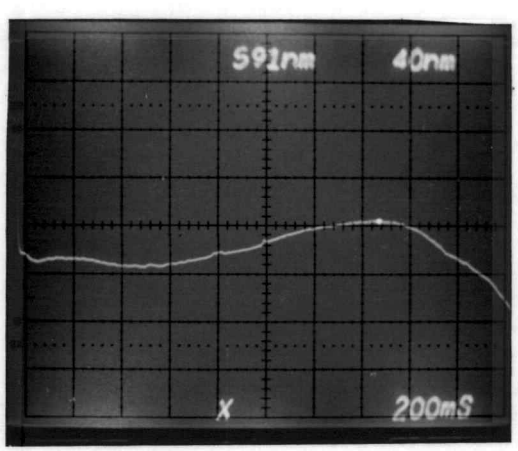

Figure 18. 300 to 700 nm emission spectrum of H_2-air combustion with ϕ = 0.69. Gain = 20.

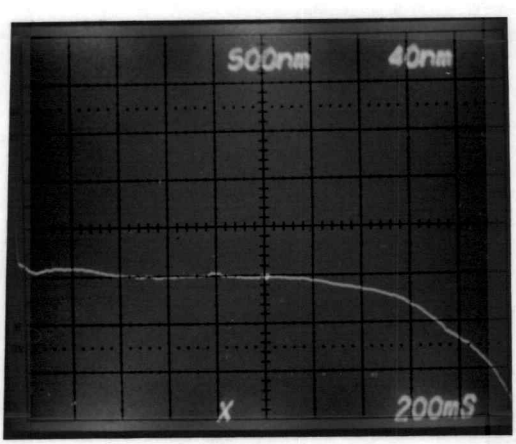

Figure 19. Zero emission trace for Figure 18.

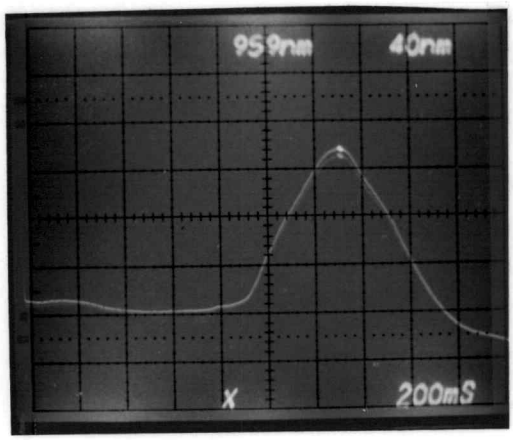

Figure 20. 700 to 1100 nm emission spectrum of H_2-air combustion with ϕ = 0.69. Gain = 5.

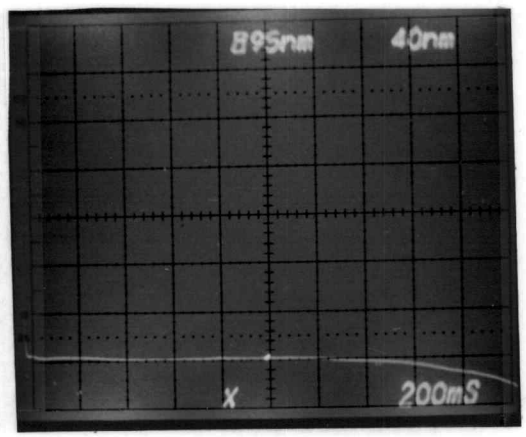

Figure 21. Zero emission trace for Figure 20.

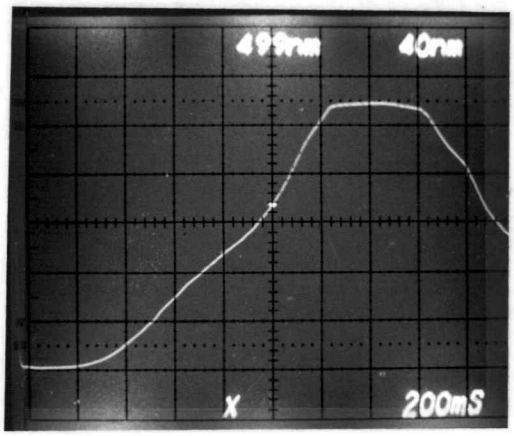

Figure 22. 300 to 700 nm emission spectrum of CO-air combustion with ϕ = 1.00. Gain = 2.

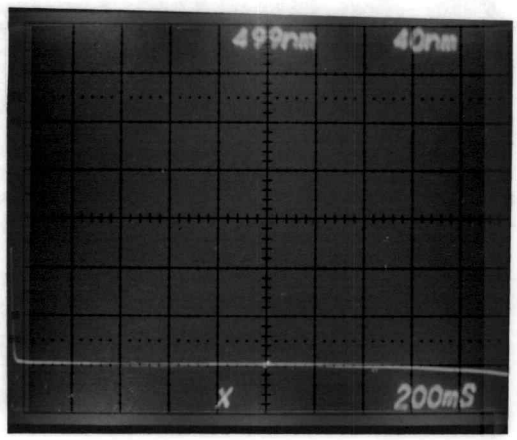

Figure 23. Zero emission trace for Figure 22.

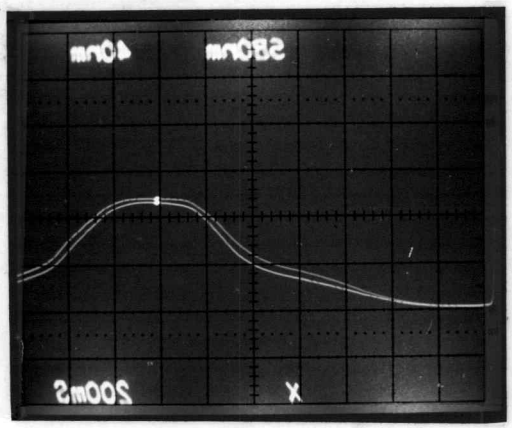

Figure 24. 300 to 700 nm emission spectrum of CO-air combustion with ϕ = 1.50. Gain = 1.

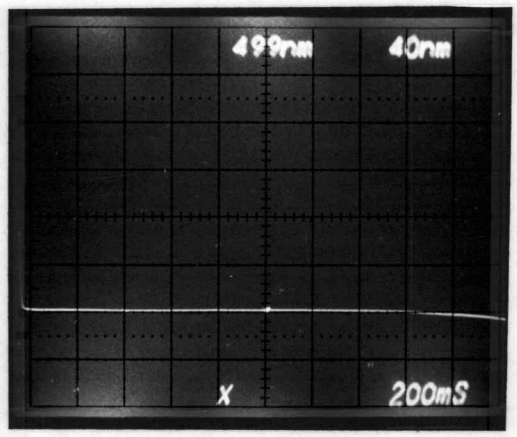

Figure 25. Zero emission trace for Figure 24.

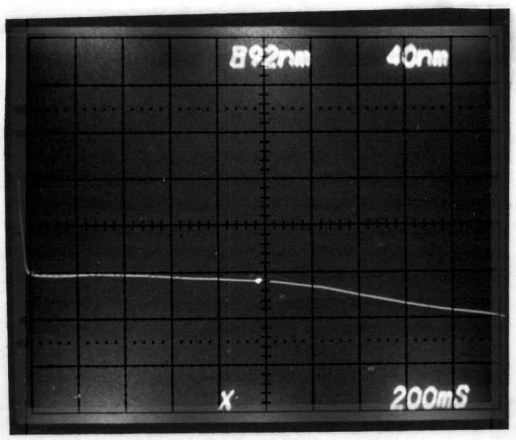

Figure 26. 900 to 1100 nm emission spectrum of CO-air combustion with ϕ = 1.50. Gain = 1.

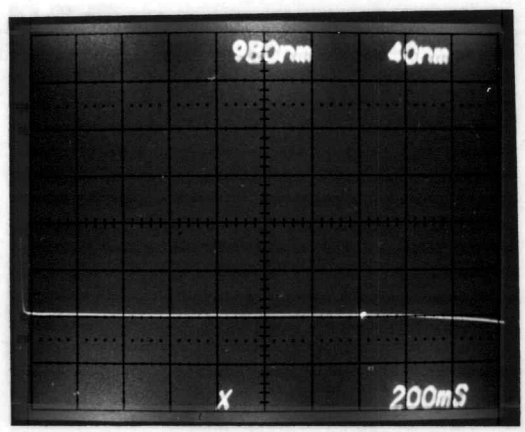

Figure 27. Zero emission trace for Figure 26.

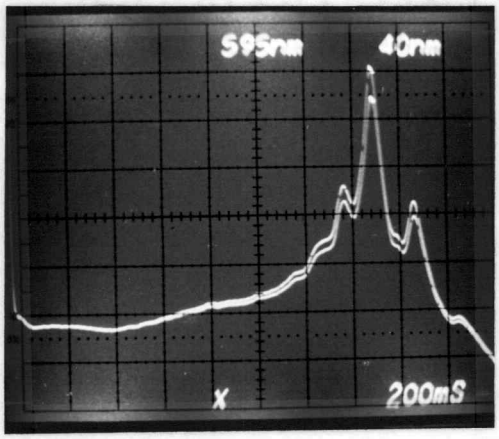

Figure 28. 300 to 700 nm emission spectrum of CO-air combustion with ϕ = 1.65. Gain = 10.

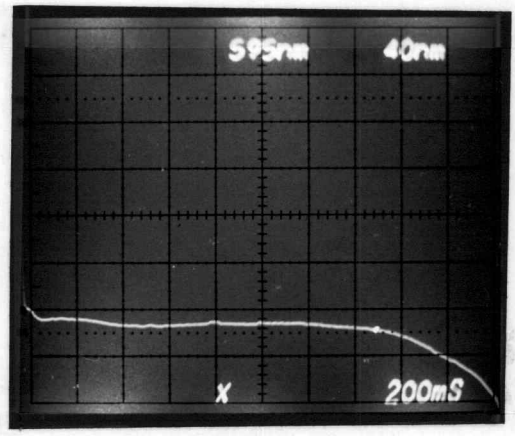

Figure 29. Zero emission trace for Figure 28.

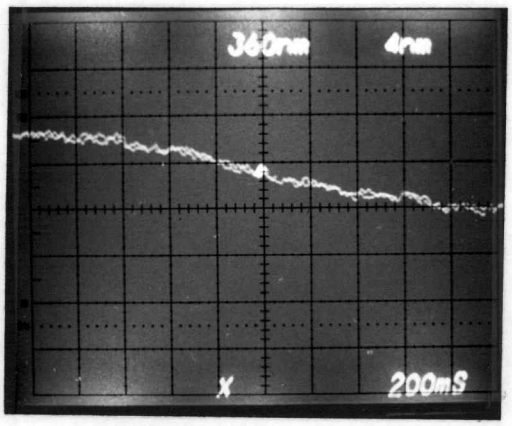

Figure 30. 340 to 380 nm emission spectrum of CO-air combustion with ϕ = 1.65. Gain = 200. showing no evidence of Dislandres d'Azambuja C_2 band system.

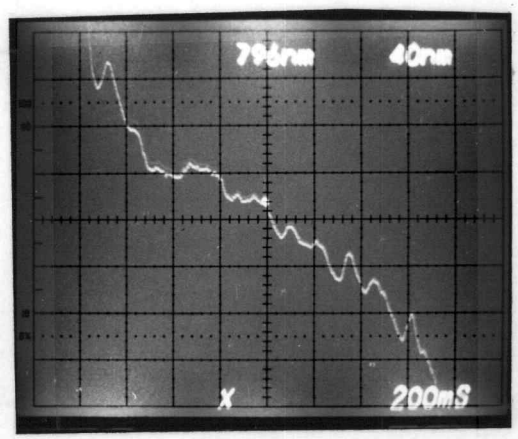

Figure 31. 600 to 1000 nm emission spectrum of CO-air combustion with ϕ = 1.65. Gain = 50. showing peaks thought to represent band heads of Phillips C_2 system.

closely with band heads at 567.0, 598.2, and 640.1.

Searching for rarer species revealed the presence of C_2. In Figure 30, no evidence of the Dislandres d'Azambuja C_2 system appears at 359.2 or 360.7 nm (17) even with Φ = 1.65 and gain set at 200. However, Figure 31 shows peaks corresponding within reasonable accuracy with those of the Phillips C_2 system, these being 771.4, 790.7, 810.8, 875.1, 898.0, and 1014.7 nm.(17) The bands were visible chiefly due to the lack of overlap from the CO and CO_2 near continuous-type spectra and the fact that Φ = 1.65.

A search for the CN and NCN radicals revealed nothing.

Again no ultraviolet readings were available, no doubt, chiefly due to the relative opacity of the glass fibre optics to the shorter wavelengths. All major components of the CO_2- air system were observable.

Hydrocarbon Fuel Emissions

As might be expected, the hydrocarbon fuel (gasoline) emissions exhibit spectral features of both hydrogen and carbon monoxide combustion. Figures 32 and 33 reveal the CO-CO_2 band "bulge" in the 400 - 600 nm range and Figures 34 and 35 show the H_2O peak at approximately 960 nm, slightly shifted from H_2-air combustion. The equivalency ratio was 0.8 and the gain was 20 for each set of photographs.

Pronounced increases in intensity resulted from an increase in Φ as illustrated in Figure 36 (vertical gain setting is 10, Φ = 1.0) and Figure 37 (vertical gain setting is 5, Φ = 1.2).

Searches were conducted for the identifying wavelength emissions for

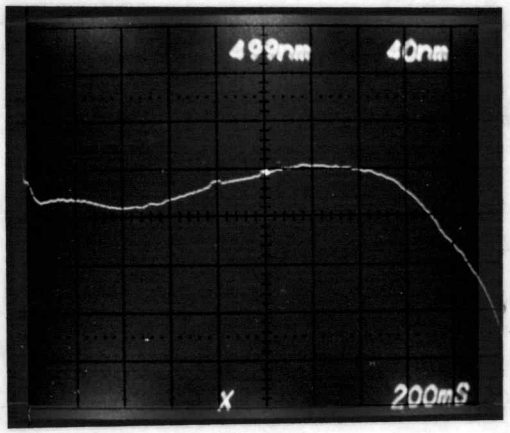

Figure 32. 300 to 700 nm emission spectrum of gasoline-air combustion with ϕ = 0.80. Gain = 20.

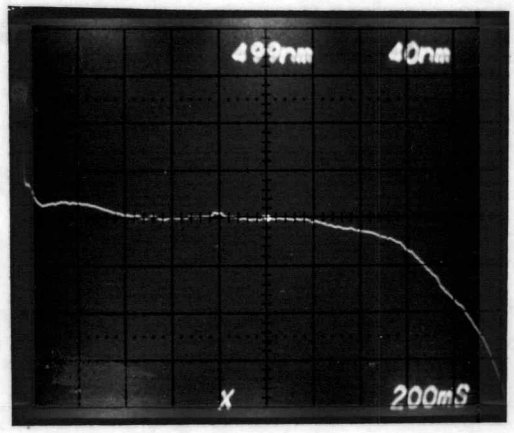

Figure 33. Zero emission trace for Figure 32.

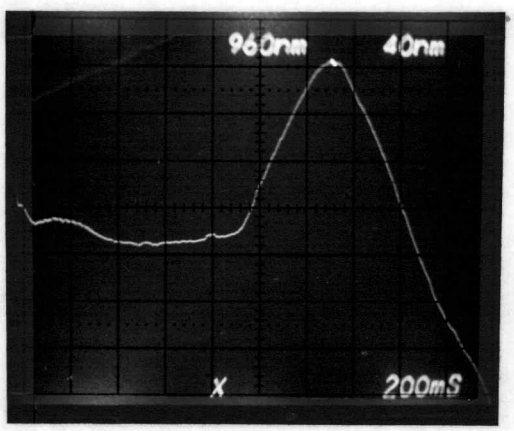

Figure 34. 700 to 1100 nm emission spectrum of gasoline-air combustion with ϕ = 0.80. Gain = 20.

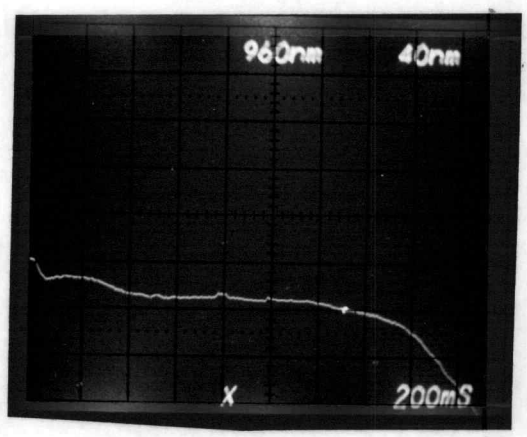

Figure 35. Zero emission trace for Figure 34.

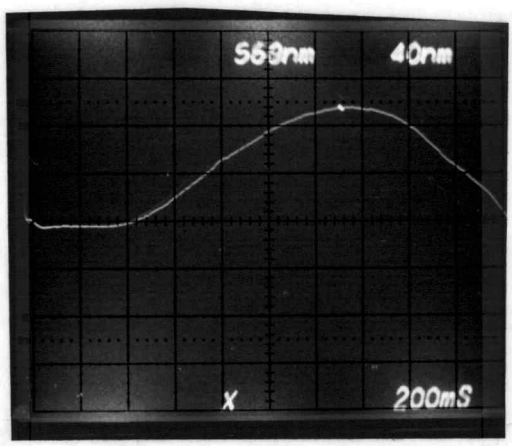

Figure 36. 300 to 700 nm emission spectrum of gasoline-air combustion with ϕ = 1.00. Gain = 10.

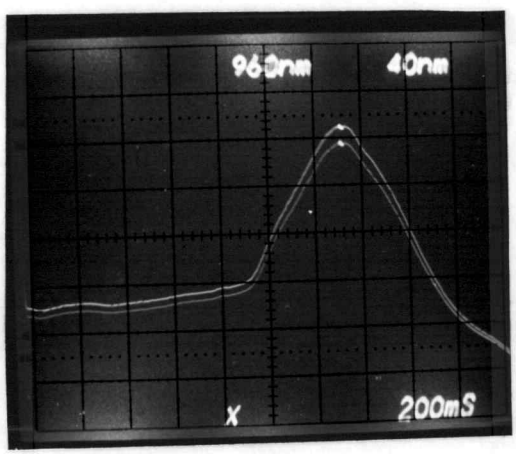

Figure 37. 700 to 1100 nm emission spectrum of gasoline-air combustion with ϕ = 1.20. Gain = 5.

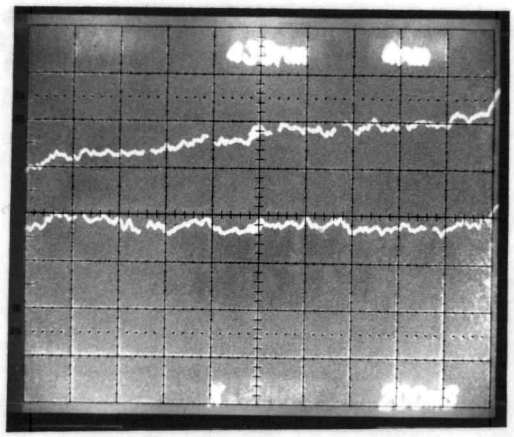

Figure 38. 413 to 453 nm emission spectrum of gasoline-air combustion with ϕ = 1.0, gain = 200 showing no emissions identifying CH radical.

CHO, CH_2O, CH, and C_2 to no avail. As most of the identifying bands lie in the 290.0 to 450.0 nm range, they were masked by both CO - CO_2 emission and the lack of ultraviolet throughout exhibited by this assembly. Figure 38 shows a stored trace photograph indicating the no light and emission traces in the 430 nm area. (This spectral section includes the 430 nm system identifying the CH radical). As can be seen, the continuum-type spectrum is prevalent here but there were no identifiable line or band systems.

CONCLUSIONS

The Tektronix Rapid Scanning Spectrometer demonstrated a capability of displaying general molecular spectra which result from the combustion processes of an internal combustion engine. The multiple band spectra of CO and CO_2 in 400 to 700 nm range and of H_2O in 900 to 1050 nm range were the most prominent spectral features. The strength of spectral output resulting from these three molecules is attributable to the relatively high concentrations in the product gases.

No line spectra were noted during this work. This is most likely due to the fact that the thermal excitation given the molecules during combustion causes sufficient vibrational spectra to hide line spectra due to electronic transitions in the component atoms. Work by Marrs and Caryl indicates that line spectra are displayed, at least for sodium, if the proper material is introduced into the combustion chamber.(26) Of course, electronic transitions may occur during combustion outside the range of the Tektronix unit.

Spectral outputs indicative of rarer molecular species, specifically, NO, OH, H_2, etc. were not apparent, though predicted thermodynamically. This was due to the masking effect of the higher concentration gases, CO, CO_2, and H_2O. Also, many identifying wavelengths were located in the near ultraviolet range where the glass fibre optic device severely limited radiation transmission. Even at high values of vertical gain, no positive identification of these rarer species was possible. Only at the long wavelength frequencies, away from the masking effects of the CO, CO_2, and H_2O bands, may individual peaks be noted.

A benefit of the RSS, especially when used in examining a continuous or repeating source of radiation, is the ability to rapidly search the entire spectrum covered by the instrument by simply turning a knob. This capability allowed very rapid searches to be made for specific spectral features. Since this investigation was based on certain suspected gases, the searches of specific frequency ranges surrounding the supposed identifying feature, were executed rapidly.

Though the RSS has rapid response and allows the operator to rapidly inspect the spectral display, some limitations became apparent from this study. Identification of molecular types in areas of high spectral density was impossible, in other words, as the instrument was used in this work resolution in these areas was inadequate. The severe overlapping of CO and CO_2 bands in the middle frequency range of this instrument hides any distinctive features of this region. An identical argument applies for the H_2O bands near 950 nm.

The sensitivity could be increased above the value used in this work by decreasing the entrance slit width of the spectrometer or selecting the "B" grating. Both of these alternatives have detracting features. A decrease in the slit width decreases total input power, requiring a boost in the required gain and consequent signal noise. Use of the "B" grating limits the observable area to wavelength interval of 40 nm. An effective increase in sensitivity may also be brought about by decreasing the sweep time for the electron beam. This would eliminate some of the radiation input and some of the band overlap. However, multiple sweeps during the combustion process results in multiple traces of various

amplitudes representing the radiated power at the time of each sweep. The result is a severely cluttered display.

Two methods to increase sensitivity without the drawbacks mentioned above are to increase the signal input, the power of the radiation source, and to link the beam sweeps to combustion events as done by Withrow and Rassweiler.(45) The source for the spectrometer is the fibre optic connector. The small dimensions of the fibre optic bundle (approximately 1.5 mm in diameter) and the quartz window severely limit the total light input to the entrance slit. In addition, a severe reduction in transmissivity occurs at the short wavelengths decreasing the signal even more in that region of the spectrum. By allowing an increased light input, the overall signal-to-noise ratio could be increased resulting in increased spectral sensitivity.

To effectively link the beam sweeps to combustion events requires control of both the beam sweep rate and beam triggering. As mentioned, selection of a time sweep slow enough to integrate all the combustion events in the cylinder causes an effective loss in sensitivity due to band overlapping. More detailed study could be accomplished by limiting the time period studied to smaller and smaller increments thus limiting the time of energy input but not the power. This would most likely require some type of light gating device capable of interrupting light input for predetermined intervals. A decreased sweep time may be used so that one sweep would read the signal stored while the gate was open then allowing the vidicon tube to be completely cleared of residual charge by several sweeps when the gate is closed. Positioning the quartz

window parallel to the flame front in combination with such a light gate would allow definitive studies of pre-combustion, combustion, and after-glow reactions.

In general, the spectrometer-oscilloscope assembly was very convenient to transport and handle. The two instruments, mounted on a roll-away cart, made installation and removal easy and the fibre optic unit eliminated alignment problems. Set-up time consisted of two or three minutes to install the quartz window and fibre optic lead and 20 minutes for engine and instrument warm-up.

Suggestions For Future Work

As a result of the test done here and conclusions made regarding the Tektronix RSS capabilities and limitations, the following suggestions are made for any future study with this unit:

1. Increase the area of transmission of the combustion chamber quartz window and optically align the spectrometer with the source of radiation. Position the window so that emissions received are parallel to the flame front.
2. Employ a light gate between the spectrometer and the source. Time the opening of the gate to ignition, crank angle, or some other convenient combustion activity.
3. Employ the logarithmic gain to emphasize small spectral peaks with respect to larger features.

BIBLIOGRAPHY

1. Agnew, W. G., J. T. Agnew, and K. Wark, Jr. "Comparison of Emission Sepctra of Low Temperature Combustion Reactions Produced in an Engine and in a Flat-Flame Burner." Sixth Symposium (International) on Combustion. Reinhold Publishing Corp., New York, 1956. p. 895 - 898.

2. _____ "Infrared Emission From Cool Flames. Stabilized Cool Flames; Engine Cool Flame Reactions; Gas Temperature Deduced from Infrared Emission." Fifth Symposium (International) on Combustion. Reinhold Publishing Corp., New York, 1955. p. 772 - 776.

3. Allen, W. B. Fibre Optics. Theory and Practice. Plenum Press, New York, 1973. Various paging.

4. American Society for Testing Materials. Tentative Method of Test for Knock Characteristics of Motor Fuels. ASTM, Philadelphia, 1939.

5. Baumeister, Theodore and Lionel S. Marks. Standard Handbook for Mechanical Engineers. McGraw-Hill Book Company, New York, 1967. p. 3 - 63.

6. Becker, K. H., D. Kley, and R. J. Norstrom. "OH* Chemiluminescence in Hydrocarbon Atom Flames." In Twelfth Symposium (International) on Combustion. The Combustion Institute, Pittsburgh, Pennsylvania, 1969. p. 405.

7. Burke, Peter. "Fast-scan Spectrometry." Research/Development. April, 1973. Technical Publishing Company, 1973. p. 24 - 27.

8. Canetlo, L. S. "Chemical Analysis of Air Pollution Sources." In "Combustion Generated Air Pollution," edited by E. S. Starkman, Plenum Press, New York, 1971. Various paging.

9. Carnahan, Brice, H. A. Luther, and James O. Wilkes. Applied Numerical Methods. John Wiley and Sons, Inc., New York, 1969. p. 321 - 329.

10. Caryl, Edward B. "List of Peaks Visible in Photographs Taken of C.F.R. Engine Combustion." Textronix, Inc., Beaverton, Oregon, 1975.

11. _____ Personal communication. Beaverton, Oregon, December 10, 1975.

12. de Galan, L. Analytical Spectrometry. Adam Hilger, Ltd., London, 1971. Various paging.

13. De Soete, G. G. "Overall Reaction Rate of NO and NO_2 Formation from Fuel Nitrogen." In Fifteenth Symposium (International) on Combustion. The Combustion Institute, Pittsburgh, Pennsylvania, 1974.

14. Gayden, A. G. Spectroscopy and Combustion Theory. Chapman and Hall, London, 1948. p. 86.

15. _____ The Spectroscopy of Flames. John Wiley and Sons, Inc., New York, 1975. p. 205 - 206.

16. Handbook of Chemistry and Physics, edited by Charles D. Hedgman, M.S. The Chemical Rubber Publishing Company, Cleveland, Ohio, 1961. p. 3114.

17. Handbook of Spectroscopy, Volume I, edited by J. W. Robinson. CRC Press, Cleveland, Ohio, 1974. p. 772 - 773.

18. Haynes, B. S., D. Iverach, N. Y. Kirov. "The Behavior of Nitrogen Species in Fuel Rich Hydrocarbon Flames." In Fifteenth Symposium (International) on Combustion. The Combustion Institute, Pittsburgh, Pennsylvania. p. 1103.

19. Hershey, A., J. Eberhardt, and H. Hottel. "Thermodynamic Properties of the Working Fluid in Internal Combustion Engines." Society of Automotive Engineers Journal, Volume 39, Number 4, 1936.

20. Herzberg, G. "Spectra of Diatomic Molecules." Van Nostrand, New York, 1950. Various paging.

21. Hottel, H. C., G. C. Williams, and C. N. Satterfield. Thermodynamic Charts for Combustion Processes. John Wiley and Sons, Inc., New York, 1949.

22. Kinney, J. R., and G. M. Reistad. S I Units and Conversions. Corvallis, Oregon, 1974.

23. Lewis, Bernard and Guenther von Elbe. "Combustion, Flames and Explosions of Gases." Academic Press, Inc., New York and London, 1961. p. 75.

24. Lichty, Luther C. Combustion Engine Processes. McGraw-Hill, New York, 1967. p. 628 - 636.

25. Malte, P. C., and D. T. Pratt. "Measurement of Atomic Oxygen and Nitrogen Oxides in Jet-Stirred Combustion." In Fifteenth Symposium (International) on Combustion. The Combustion Institute, Pittsburgh, Pennsylvania, 1974. p. 1061.

26. Marrs, Jere M. "Measurement of Spectra in Internal Combustion Engine Cylinders." Tektronix, Inc., Beaverton, Oregon, 1975.

27. _____ "Rapid Color Measurement." In Research/Development. Technical Publishing Company, 1974. p. 22 - 26.

28. _____ "Stopped-Flow Kinetics Using the Tektronix J20/7J20 Rapid Scan Spectrometer and the Durrum Kinetic Spectrophotometer." In Rapid Scan Spectrometry Application Notes. Tektronix, Inc., Beaverton, Oregon, October, 1973.

29. _____ and E. B. Caryl. Personal communication. Corvallis, Oregon, February 1, 1975.

30. Newhall, Henry K. "Kinetics of Engine Generated Nitrogen Oxides and Carbon Monoxide." Twelfth Symposium (International) on Combustion. The Combustion Institute, Pittsburgh, Pennsylvania, 1969. p. 604.

31. _____ "Theoretical and Experimental Investigation of Chemical Kinetics During Rapid Expansion of High Temperature Combustion Products." Doctoral Thesis, University of California, Berkeley, California, 1966. Various paging.

32. Norrish, R. G. W. "The Study of Combustion by Photochemical Methods." In Tenth Symposium (International) on Combustion. The Combustion Institute, Pittsburgh, Pennsylvania, 1965. p. 10.

33. Obert, Edward F. Internal Combustion Engines. International Textbook Company, Scranton, Pennsylvania, 1968. Various paging.

34. Rose, R. A., G. C. Wilson, and R. R. Benedict. "Photo-Electric Combustion Analysis." SAE Transactions, SAE, Inc., New York, November, 1936.

35. Shore, Bruce W., and Donald H. Menzel. Principles of Atomic Spectra. John Wiley and Sons, New York, 1968. Various paging.

36. Sienko, Michell J., and Robert A. Plane. Chemistry. McGraw-Hill Book Company, New York, 1966. p. 50 - 59.

37. Smith, J. M., and H. C. Van Ness. Introduction to Chemical Engineering Thermodynamics. McGraw-Hill, New York, 1959. p. 423.

38. Starkman, E. S. "Theory Experiment and Rationale in the Generation of Pollutants by Combustion." Twelfth Symposium (International) on Combustion. The Combustion Institute, 1969. p. 594 - 598.

39. Tektronix Oscilloscope Camera System. Tektronix, Inc., Beaverton, Oregon, 1971. Various paging.

40. "Tektronix J20/7J20 Rapid-Scanning Spectrometer Operators Instruction Manual." Tektronix, Inc., Beaverton, Oregon, March, 1974. Various paging.

41. "Tektronix, J20/7J20 Rapid Scanning Spectrometer Service Instruction Manual." Tektronix, Inc., Beaverton, Oregon, 1974. p. 1-1 through 2-8.

42. "Tektronix 7313/RT313 Oscilloscope Interim Instruction Manual." Tektronix, Inc., Beaverton, Oregon, 1973. Various paging.

43. Tektronix, Inc. "Test Response Curve of the J20/7J20 Rapid Scanning Spectrometer." Tektronix, Inc., Beaverton, Oregon, October 4, 1973.

44. Van Wylen, Gordon J., and Richard E. Sonntag. Fundamentals of Classical Thermodynamics. John Wiley and Sons, 1965. p. 618.

45. Withrow, Lloyd, and Gerald M. Rassweiler. "Slow Motion Shows Knocking and Non-knocking Explosions." SAE Transactions, SAE, Inc., New York, 1936.

46. _____ "Studying Engine Combustion by Physical Methods, A Review." In "Journal of Applied Physics." Volume 9, Number 6, June, 1938. p. 365 - 366.

APPENDIX

Table A-I. Air - Fuel Flow Calibration

Air Temperature = 298°K

Fuel Type	Fuel Meter Reading (% Max Flow)	Fuel Flow Rate 10^{-3} m/s	Air Meter Reading 10^{-2} m	Air Flow Rate 10^{-3} m/s	STOIC F/A	Φ
H_2		0.130				
H_2	35.5	0.260	1.397	2.305	0.420	0.269
H_2	65	0.523	1.143	2.085	0.420	0.597
H_2	70	0.571	0.939	1.889	0.420	0.719
CO	50	0.582	0.990	1.940	0.420	0.714
CO	66	0.769	0.889	1.838	0.420	0.996
CO	70	0.816	0.762	1.702	0.420	1.141
CO	86	1.000	0.635	1.554	0.420	1.532
CO	103	1.200	0.508	1.390	0.420	2.055
None	0		1.470	2.364		

Measured volumetric efficiency = 78.8%

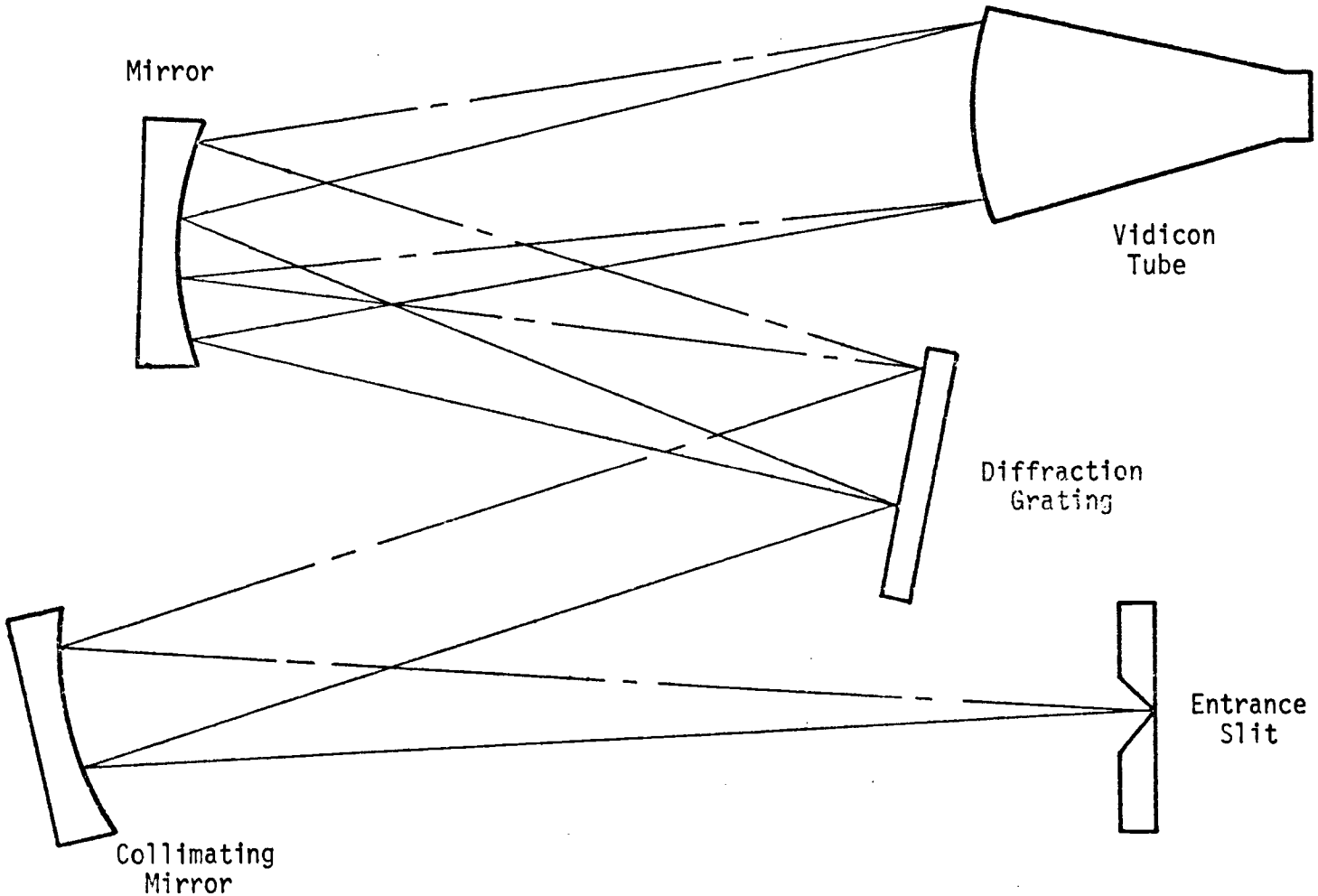

Figure A-1. Schematic of Czerny-Turner spectrometer mounting as used in Tektronix RSS. (26)

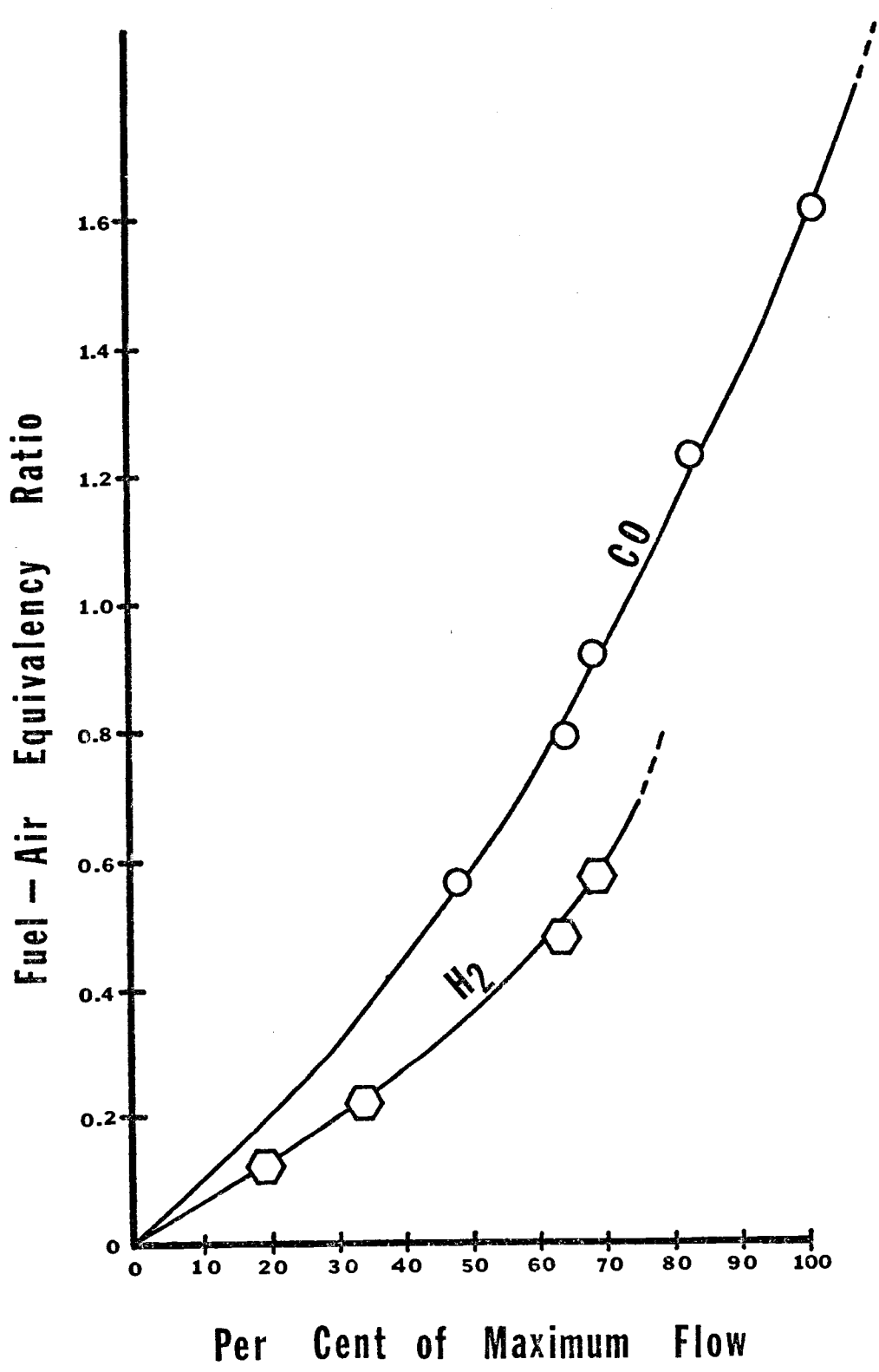

Figure A-2. Gaseous fuel calibration curves for fuel-air equivalency ratio versus per cent of maximum flowmeter reading.

Table A-II. Fuel - Air Ratio Calibration Data For Gasoline

Air Temperature = 297°K

Air Flow Meter Reading = 1.62×10^{-3} m of H_2O

Fuel Quantity Used (10^{-6} m^3)	Time of Flow (s)	Fuel Column Height (10^{-2} m below venturi centerline)	F/A Ratio	Φ
59.0	120	0	0.126	1.638
71.4	180	1.27	0.110	1.430
59.6	180	2.54	0.085	1.105
29.3	105	3.81	0.071	0.923
46.9	190	5.08	0.063	0.819
56.5	255	6.35	0.056	0.728
37.6	195	7.62	0.049	0.637
26.8	120	6.35	0.057	0.741
23.2	120	7.62	0.049	0.637
59.9	140	1.27	0.109	1.417
81.2	45	0	0.126	1.638

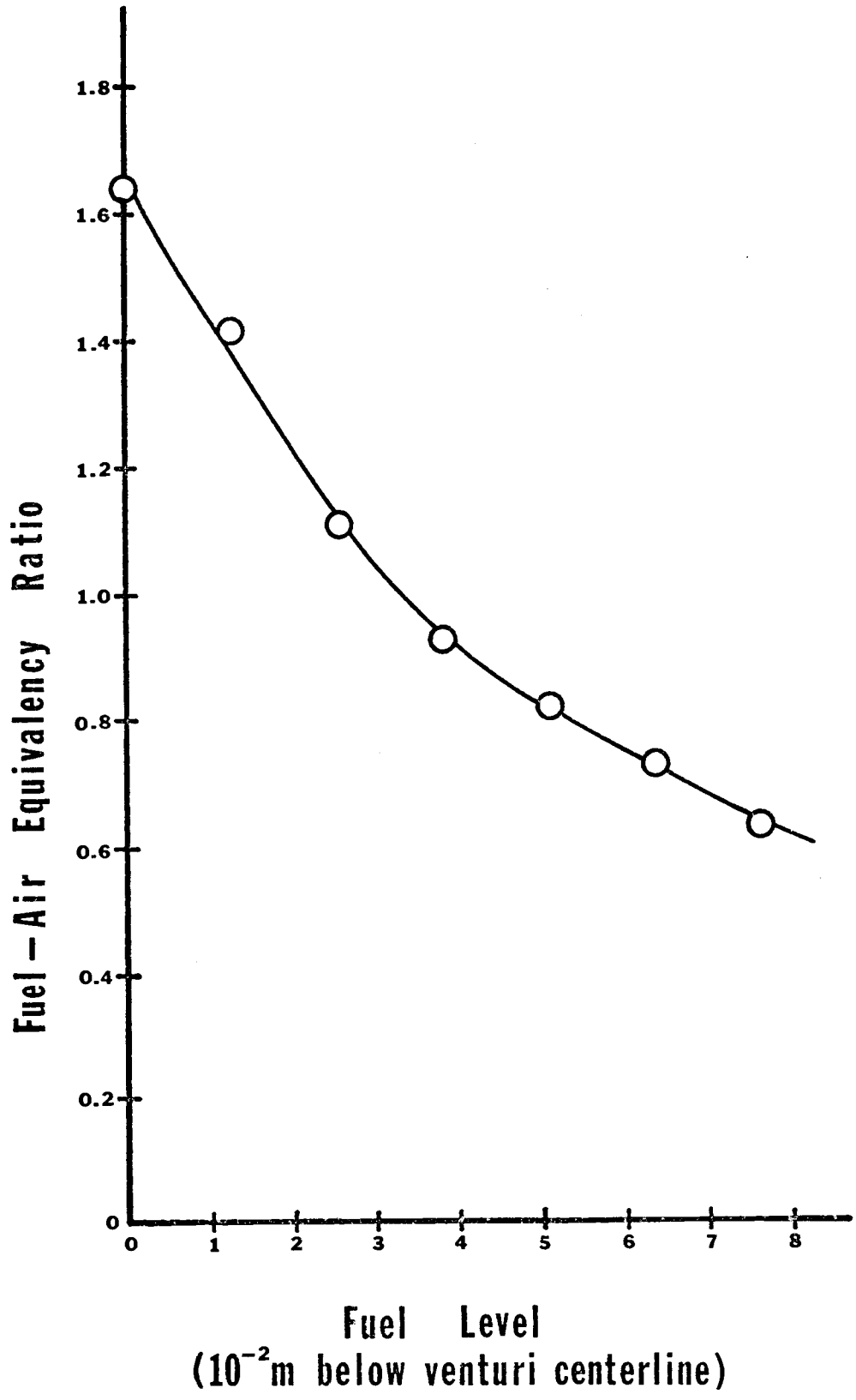

Figure A-3. Gasoline calibration curve for fuel-air equivalency ratio versus distance of fuel level below venturi centerline.

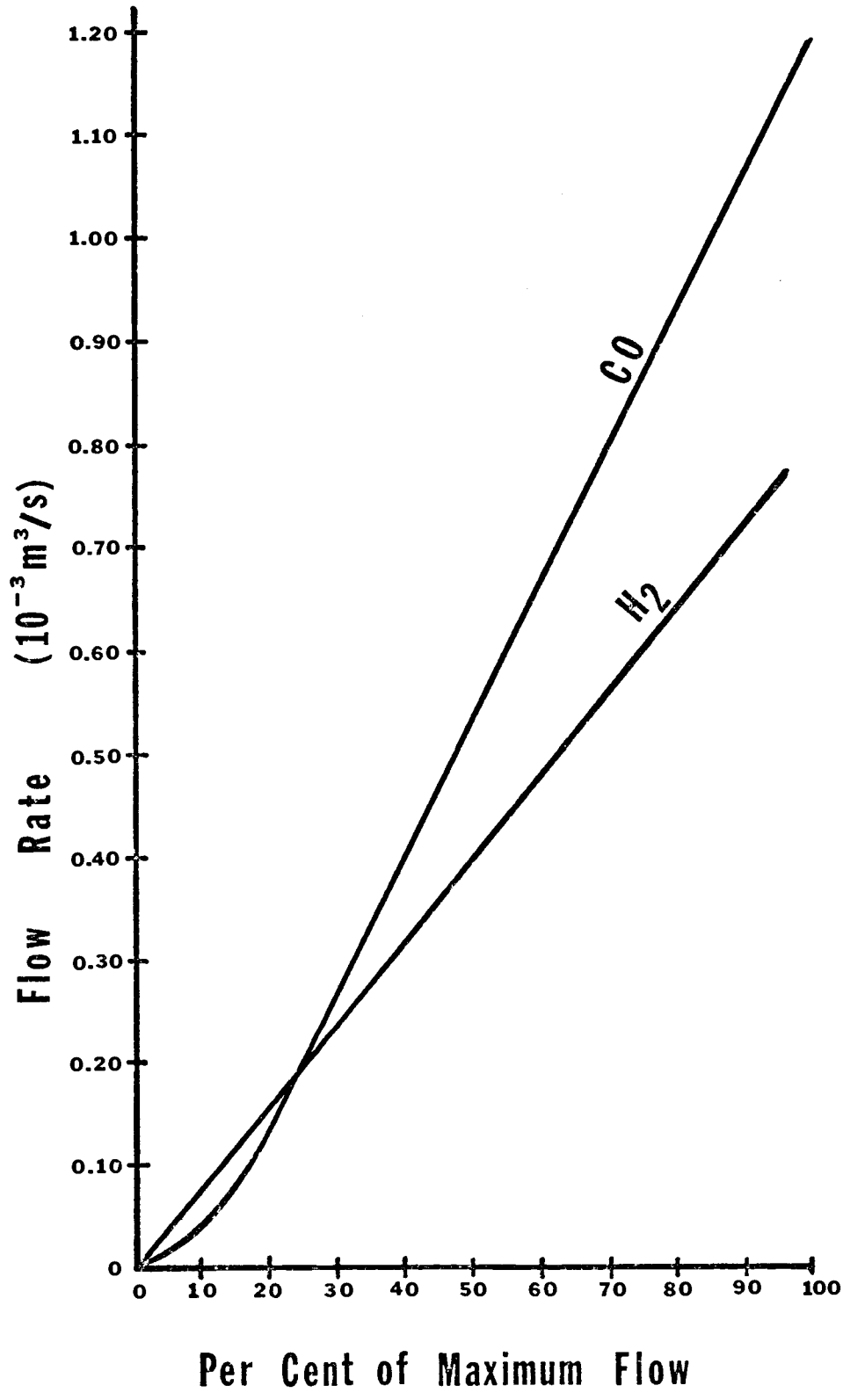

Figure A-4. Calibration curves for actual flow versus per cent of maximum flowmeter reading.

DETERMINATION OF AIR FLOW

(1) Estimation of air meter nozzle Reynold's no.

$$Q = 1/2 \times 600 \times 10^{-6}\ m^3 \times 10\ \left(\frac{\text{revolutions}}{s}\right) = 3.0 \times 10^{-3}\ m^3/s$$

Assuming 80% volumetric efficiency

$$Q = 0.8 \times 3.0 \times 10^{-3}\ m^3/s = 2.4 \times 10^{-3}\ m^3/s$$

For a 2.542×10^{-2} m diameter nozzle throat, the average velocity is

$$V_{avg.} = \frac{2.4 \times 10^{-3}\ m^3/s}{(2.542 \times 10^{-2}\ m)^2\ \pi/4} = 4.729\ m/s$$

Therefore, the Reynold's number at 298°K is

$$\text{Re no.} = \frac{\rho\ V_{avg.}\ d}{\mu} = \frac{1.20\ Kg/m^3\ \ 4.729\ m/s\ \ 2.542 \times 10^{-2}\ m}{1.824 \times 10^{-5}\ Kg/m \cdot s}$$

$$= 7908.6$$

From Mark's (5) for Re = 8000, the discharge coefficient, $C_D = 0.95$

(2) Flow in terms of pressure drop across inlet nozzle

$$Q = \text{Area}_{nozzle}\ C_D\ V_{avg.}$$

$$= A_{nozzle}\ C_D\ [2\Delta P/\rho]^{1/2}$$

$$= 5.077 \times 10^{-4}\ m^2\ (0.95) \times$$

$$\frac{[2(\Delta H\ m_{H_2O})\ 9.806 \times 10^3\ Pa/m_{H_2O}]^{1/2}}{1.204\ Kg/m^3}$$

$$Q = 6.1 \times 10^{-2}\ (\Delta H\ m_{H_2O})^{1/2}\ m^3/s$$

SAMPLE CALCULATION OF PRODUCTS OF COMBUSTION

Assumptions

Gasoline was assumed to be octane, (chemical formula C_8H_{18}) to be burned with the stoichoimetric amount of air. (Φ = 1.0). The CFR engine was adjusted to a compression ratio of 6.0:1 and a volumetric efficiency of 80% was assumed. The products of combustion must be assumed. An accurate original guess of the major product gases is most helpful in rapidly reaching the final composition, therefore, the original, overall chemical equation is guessed as:

$$C_8H_{18} + 12.5\ O_2 + 47\ N_2 = 8.5\ H_2O + 1.2\ CO + 6.8\ CO_2 \qquad \text{(Eq. 1)}$$
$$+ 47\ N_2 + 0.5\ X$$

These reactions indicate compositions as follows:

H_2O	0.13281	CO_2	0.10625
CO	0.01875	N_2	0.73438
		Other (X)	0.00781

Equations

From the overall chemical reaction, a peak temperature may be estimated. First the energy release, due to constant volume combustion, is calculated from:

$$\Delta U_{reaction} = \sum_{PRODUCTS} n_i u_i - \sum_{REACTANT} n_i u_i \qquad \text{(Eq. 2)}$$

however, for an ideal gas

$$\Delta U = \Delta H - R\Delta t$$

so that for this example,

$$\Delta U_{reaction} = \Delta H_{reaction} - R\Delta t_{reaction}$$

$$\Delta H_{reaction} = [n_{H_2O}(h_{H_2O}) + n_{CO}(h_{CO}) + n_{CO_2}(h_{CO_2}) + n_{N_2}(h_{N_2})] - [n_{C_8H_{18}}(h_{C_8H_{18}}) + n_{O_2}(h_{O_2}) + n_{N_2}(h_{N_2})] \quad \text{(Eq. 3)}$$

$$\Delta H = [8.5\ (-2.418 \times 10^5\ \text{J/mol}) + 1.2\ (-1.105 \times 10^{-5}) + 6.8\ (-3.935 \times 10^{-5}) + 47\ (0)] - [1.0\ (-2.499 \times 10^5) + 12.5\ (0) + 47\ (0)]$$

$$= -4.614 \times 10^6\ \text{J/mol octane}$$

Therefore, ΔU must now be calculated using an estimated Δt. Guessing Δt as 2400°K, the change in internal energy is calculated as

$$\Delta U = \Delta H - R\Delta T = -4.614 \times 10^6\ \text{J/mol} - (8.314\ \text{J/mol} \cdot \text{K}\ (2400°\text{K})$$

$$= -4.634 \times 10^6\ \text{J/mol}$$

Second, this energy output of the reaction is used in an energy balance equation to obtain the peak temperature.

$$\left[\sum_{PRODUCTS} n_i\ C_{vi}\right](t-273) - \Delta H_{reaction} = 0 \quad \text{(Eq. 4)}$$

Of necessity, the equation above is solved iteratively, since the specific heat values, C_{vi}, for individual product gases are a function of temperature.

Expanding Equation 4 for the assumed product gases of the example gives

$$[8.5\ (C_{vH_2O}) + 1.2\ (C_{vCO}) + 6.8\ (C_{vCO_2}) + 47\ (C_{vN_2})]\ (t_{max}-273) - 4.634 \times 10^6 = 0 \quad \text{(Eq. 5)}$$

The value of t_{max} is again assumed, the C_v values calculated, and Equation 5 is solved. For this example, for the guesses of t_{max} below, the values of Equation 5 are found.

t_{max} guess	Value of (Eq. 5)
2600 K	-1.278×10^5 J/mol
2700 K	8.303×10^5 J/mol

Since linear interpolation would indicate t_{max} = 2600 K, the original Δt of 2400 K appears to have been reasonably accurate.

Assuming ideal gas relationships and, for convenience, letting t_{max} = 2700°K, the mass of the product gases in the cylinder is computed.

$$m = \frac{(3.025 \times 10^{-2}\ \text{Kg/mol})\ 8.106 \times 10^4\ \text{Pa}\ (6.14 \times 10^{-4}\ \text{m}^3)}{8.314\ \text{J/mol} \cdot \text{K}\ (297\ \text{K})}$$

$$= 6.097 \times 10^{-4}\ \text{Kg}$$

From the estimated temperature and assumed composition the peak pressure is calculated as follows:

$$P_{max} = \frac{(6.097 \times 10^{-4}\ \text{Kg})\ 8.314\ \text{J/mol} \cdot \text{K}\ (2700\ \text{K})}{2.829 \times 10^{-2}\ \text{Kg/mol}\ (1.0 \times 10^{-4}\ \text{m}^3)\ 1.013 \times 10^5\ \text{Pa/atm}}$$

$$= 47.74\ \text{atmosphere}$$

Using brackets ([]) to designate partial pressures, assuming equilibrium conditions exist, and letting A represent the number of O_2 molecules per C atom, the following equations and equilibrium constants apply:

$$1/2\ H_2 = H \qquad (K_1) \qquad \text{(Eq. 6)}$$

$$1/2\ O_2 = O \qquad (K_2) \qquad \text{(Eq. 7)}$$

$$2\ H_2O = 2\ H_2 + O_2 \qquad (K_3) \qquad \text{(Eq. 8)}$$

$$H_2O = OH + 1/2\ H_2 \qquad (K_4) \qquad \text{(Eq. 9)}$$

$$CO_2 + H_2 = CO + H_2O \qquad (K_5) \qquad \text{(Eq. 10)}$$

$$1/2\ N_2 + 1/2\ O_2 = NO \qquad (K_6) \qquad \text{(Eq. 11)}$$

$$H_2O + 1/2\ N_2 = H_2 + NO \qquad (K_7) \qquad \text{(Eq. 12)}$$

For the given estimated hydrocarbon makeup, the carbon to nitrogen and hydrogen to nitrogen balances of the product gases are:

$$[CO_2] + [CO] = ([N_2] + 1/2\ [NO])/3.76A \qquad \text{(Eq. 13)}$$

$$[H_2O] + [H_2] + 1/2\ ([H] + [OH]) = (9/8)\ ([N_2] + 1/2\ [NO])/3.76A \qquad \text{(Eq. 13a)}$$

Since air is the oxidizing agent for the combustion reaction, the O_2 to N_2 ratio of air must be satisfied. Therefore,

$$[CO_2] + [O_2] + 1/2\ ([OH] + [O] + [NO] + [H_2O] + [CO] = ([N_2] + 1/2\ [NO])/3.76 \qquad \text{(Eq. 14)}$$

Finally, the partial pressures must sum to equal the total pressure in the cylinder.

$$[N_2] + [NO] + [CO] + [CO_2] + [OH] + [H_2O] + [O_2] + [O] + [H] = P \qquad \text{(Eq. 15)}$$

Manipulation of Equations 7 through 13 lead to the following equations:

$$[H_2O] = \frac{3.76A\ [N_2] - [H_2] - \frac{K_1}{2}\ [H_2]^{1/2}}{1 + \frac{K_4}{2\ [H_2]} + \frac{9/8\ K_7\ [N_2]^{1/2}}{7.52\ A\ [H_2]}} \qquad \text{(Eq. 16)}$$

$$[NO] = \frac{K_7\ [H_2O]\ [N_2]^{1/2}}{[H_2]} \qquad \text{(Eq. 17)}$$

$$[CO] = \frac{K_5\ [H_2]\ ([N_2] + [NO]/2\ )}{3.76\ A\ ([H_2O] + K_5\ [H_2])} \qquad \text{(Eq. 18)}$$

$$[CO_2] = \frac{1\ \ [CO]\ [H_2O]}{K_5\ \ \ [H_2]} \qquad \text{(Eq. 19)}$$

$$[O_2] = K_3\ \frac{([H_2O])}{([H_2\ ])} \qquad \text{(Eq. 20)}$$

$$[OH] = K_4\ \frac{[H_2O]^{1/2}}{[H_2\ ]} \qquad \text{(Eq. 21)}$$

$$[O] = K_2 [O_2]^{1/2} \quad \text{(Eq. 22)}$$

$$[H] = K_1 [H_2]^{1/2} \quad \text{(Eq. 23)}$$

Solution of Equations

The partial pressure of N_2 is set and that of H_2 is estimated. The partial pressure of H_2O is calculated using Equation 16, then [NO] using Equation 17, and [CO] using Equation 18. The partial pressures of CO_2, O_2, OH, O, H may be calculated in any order by use of Equations 19 through 23.

Using Equation 14, the oxygen-nitrogen ratio is checked as is the total pressure using Equation 15. To correct the O_2-N_2 balance, adjust the $[H_2]$ value as needed. Correction of total pressure is accomplished by varying the $[N_2]$ value. (It was found convenient during the iteration process to graph the difference between the left and right sides of the oxygen-nitrogen balance equation versus the partial pressure of H_2 to best select the next $[H_2]$ value.)

The composition for this example is solved in five iterations below.

Species Type	Iteration Number 1	2	3	4	5	Composition
H_2O	6.121	6.223	6.227	6.2301	6.2299	0.13026
NO	0.224	0.249	0.259	0.2650	0.2644	0.00553
CO	1.004	0.942	0.912	0.8944	0.8961	0.01874
O	0.074	0.015	0.016	0.0162	0.0162	0.00034
OH	0.394	0.417	0.425	0.4307	0.4302	0.00899
CO_2	4.801	4.951	4.982	5.0005	4.9987	0.10451
O_2	0.215	0.260	0.281	0.2948	0.2935	0.00614
N_2	34.000	34.500	34.500	34.5000	34.5000	0.72133
H_2	0.200	0.185	0.178	0.1740	0.1744	0.00365
H	0.026	0.025	0.025	0.0245	0.0245	0.00051
balance	-0.148	-0.075	-0.028	0.0028	-0.00007	
Pressure	47.095	47.767	47.805	47.8302	47.8279	1.00000

Checking the composition results against the original chemical equation (Eq. 1) shows good agreement and the total pressure is within 0.2 per cent of the previously determined value.

For combustion of H_2-air mixtures, Equations 6, 7, 8, 9, 12, 13a, 16, 17, 20 - 23 are used and Equations 14, and 15 are modified to eliminate the carbon component gases. The O_2 to C ratio, A, is substituted for by the quantity 9/8 (O_2/H_2).

For the combustion of CO-air mixtures, the following reaction is considered:

$$x\ CO + yO_2 + 3.76\ yN_2 = CO + CO_2 + N_2 + O_2 + NO + O + C \qquad \text{(Eq. 24)}$$

The nitrogen to carbon ratio is then:

$$B = \frac{N_2}{C} = \frac{3.76\ y}{x}$$

and the oxygen to nitrogen ratio for the reactants is:

$$D = \frac{O_2}{N_2} = \frac{y + x/2}{3.76y}$$

Additional equilibrium equations which apply are:

$$C + 1/2\ O_2 = CO \quad (K_8) \qquad \text{(Eq. 25)}$$

$$CO + 1/2\ O_2 = CO_2 \quad (K_9) \qquad \text{(Eq. 25)}$$

plus Equations 7 and 11.

The species balance equations become:

For C to N_2

$$[C] + [CO_2] + [CO] = 1/B\ ([N_2] + 1/2\ [NO]) \qquad \text{(Eq. 26)}$$

and for O_2 to N_2

$$O_2 + CO_2 + 1/2\ ([O] + [CO] + [NO]) = D\ ([N_2] + 1/2\ [NO]) \qquad \text{(Eq. 27)}$$

Equation 15 is modified to eliminate component gases containing hydrogen and to add carbon gas.

The procedure for solution is:

1. Set partial pressure of N_2; $[N_2]$
2. Guess partial pressure of O_2; $[O_2]$
3. Calculate

$$[NO] = K_4\ ([O_2]\ [N_2])^{1/2} \qquad \text{(Eq. 28)}$$

$$[CO] = \frac{1/B\ ([N_2] + [NO]/2)}{1 + K_9\ [O_2]^{1/2} + \frac{1}{K_8\ [O_2]^{1/2}}} \qquad \text{(Eq. 29)}$$

$$[CO_2] = K_9\ [CO]\ [O_2]^{1/2} \qquad \text{(Eq. 30)}$$

$$[O] = K_3\ [O_2]^{1/2} \qquad \text{(Eq. 31)}$$

$$[C] = \frac{[CO]}{K_8\ [O_2]^{1/2}} \qquad \text{(Eq. 32)}$$

4. Balance Equations 27 and 15
5. Adjust assumed $[O_2]$ and $[N_2]$ values and repeat calculation step 3.

The balancing of Equations of 27 and 15 above follows the same iterative procedure as for hydrocarbon combustion.

Table A-III. Photographic Log - Roll Number 1

Frame No.	Fuel Type	Spectrum Range Displayed (nm)	Φ Value or % Max. Flow	Remarks	Slit Width	Vertical Gain
1	None	300 - 700	----	Baseline Trace	Open	10
2	Gasoline	300 - 700	.8	No Light	Open	20
3	Gasoline	300 - 700	.8	---	Open	20
4	Gasoline	700 - 1100	.8	No Light	Open	20
5	Gasoline	700 - 1100	.8	Firing	Open	20
6	Gasoline	700 - 1100	.8	No Fire	Open	20
7	Gasoline	700 - 1100	.8	Firing	Open	20
8	Gasoline	300 - 700	1.0	No Light	Open	10
9	Gasoline	300 - 700	1.0	Firing	Open	10
10	Gasoline	700 - 1100	1.0	No Fire	Open	5
11	Gasoline	700 - 1100	1.0	Firing	Open	5
12	Gasoline	300 - 700	1.2	No Light	Open	10
13	Gasoline	300 - 700	1.2	Firing	Open	10
14	Gasoline	700 - 1100	1.2	No Light	Open	5
15	Gasoline	700 - 1100	1.2	Firing	Open	5
16	Gasoline	700 - 1100	1.2	No Fire	Open	5
17	Gasoline	700 - 1100	1.2	Firing	Open	5
18	CO	300 - 700	65%	No Light	Open	1
19	CO	300 - 700	65%	Firing	Open	1
20	CO	700 - 1100	65%	No Light	Open	1
21	CO	700 - 1100	65%	Firing	Open	1
22	CO	300 - 700	85%	No Light	Open	1
23	CO	300 - 700	85%	Firing	Open	1
24	CO	900 - 1100	85%	No Light	Open	1
25	CO	900 - 1100	85%	Firing	Open	1
26	CO	300 - 700	85%	No Light	Open	1
27	CO	900 - 1100	85%	No Light	Open	1
28	H_2	300 - 700	35%	No Light	Open	20
29	H_2	300 - 700	35%	Firing	Open	20
30	H_2	700 - 1100	35%	Firing	Open	20

Table A-III. Photographic Log - Roll Number 2

Frame No.	Fuel Type	Spectrum Range Displayed (nm)	Φ Value or % Max. Flow	Remarks	Slit Width	Vertical Gain
1	H_2	500 - 900	59%	Light	Open	10
2	H_2	500 - 900	59%	Not Firing	Open	10
3	--	---	---	---	---	--
4	H_2	300 - 700	59%	No Light	Open	20
5	H_2	300 - 700	59%	Firing	Open	20
6	H_2	700 - 1100	59%	No Light	Open	20
7	H_2	700 - 1100	59%	No Light	Open	20
8	H_2	700 - 1100	59%	No Light (Repositioned)	Open	10
9	H_2	700 - 1100	59%	Firing	Open	10
10	H_2	300 - 700	69%	No Light	Open	20
11	H_2	300 - 700	69%	No Light	Open	20
12	H_2	300 - 700	69%	Firing	Open	20
13	H_2	700 - 1100	69%	No Light	Open	5
14	H_2	700 - 1100	69%	Firing	Open	5
15	CO	300 - 700	66%	No Light	Open	2
16	CO	300 - 700	66%	No Light	Open	2
17	CO	300 - 700	66%	Firing	Open	2
18	CO	300 - 700	66%	Firing	Open	2
19	CO	700 - 1100	66%	Firing (same base as 15)	Open	2
20	H_2	917 - 957	59%	No Fire	200	100
21	H_2	917 - 957	59%	Firing	200	100
22	CO	300 - 700	89%	Firing	200	10
23	CO	Zero	89%	22	200	10
24	CO	480 - 520	86%	Firing	200	20
25	CO	340 - 380	89%	Firing - Showing no C	200	200
26	CO	366 - 406	89%	Firing - No CN	200	50
27	CO	700 - 1100	89%	Firing - No CN	200	50
28	CO	497 - 897	89%	Firing	200	20
29	CO	596 - 996	89%	Firing	200	50
30	CO	1044 - 1100	89%	Firing - No change when firing	200	50

Table A-III. Photographic Log - Roll Number 3

Frame No.	Fuel Type	Spectrum Range Displayed (nm)	Φ Value or % Max. Flow	Remarks	Slit Width	Vertical Gain
1	Gasoline	300 - 700	1.2	Showing pk. at 592 after sev. fire	200	50
2	Gasoline	300 - 700	1.2	Not Firing	200	50
3	Gasoline	450 - 550	1.2	Showing no C	200	50
4	Gasoline	800 - 0	1.2	Firing	200	50
5	Gasoline	800 - 0	1.2	Not Firing	200	50
6	Gasoline	700 - 1100	.8	Firing	200	100
7	Gasoline	700 - 1100	.8	Not Firing	200	100
8	Gasoline	233 - 633	1.0	Firing CH area	200	200
9	Gasoline	366 - 406	1.0	Firing CH area	200	200
10	Gasoline	394 - 334	1.0	Firing CH area	200	200
11	Gasoline	375 - 415	1.0	Firing CH_2O area	200	200
12	Gasoline	1070 - 1100	1.0	CN Check	200	20
13	Gasoline	894 - 934	1.0	CN Check	200	100
14	Gasoline	300 - 304	.8	OH Check	200	200
15	None	400 - 800		No Light	200	100
16	None	400 - 800		Fluorescent Light	200	100